



Deutsches Zentrum
für Luft- und Raumfahrt

Institut für
Vernetzte Energiesysteme



**Carl von Ossietzky Universität
Oldenburg**

Institute of Physics

&

German Aerospace Center (DLR)

Institute of Networked Energy Systems

Master Thesis

**The German Northwestern Grid
Modelling & Transient Stability:
Virtual Synchronous Machines
(VSMs) Penetration**

Ahmad Allahham

Time frame: Feb. 2023 - August 2023

Supervisor

Dorothee Peters

Examiners

Prof. Dr. Carsten Agert

Frank Schuldt

Abstract

This thesis focuses on the modelling of the German grid. The Northwestern grid is implemented into more details. It also focuses on the assessment of transient stability. Two demand scenarios are considered: one representing the maximum demand within Germany and another encompassing the maximum demand including loads outside Germany. Various scenarios involving large disturbances are examined to evaluate the transient stability of the grid. The study employs RMS simulation techniques to analyze the system's performance under different conditions. Tools like Python, Matlab/ Simulink, and PowerFactory will be used in data analysis, dynamic models building, and simulation, respectively.

The investigation includes an analysis of the existing control mechanisms employed in renewable energy sources, as well as the integration of grid-forming controllers such as virtual synchronous machines (VSMs) and Synchronverters. The stability of the system is compared when utilizing currently used controllers in inverter-based resources and when employing VSMs and Synchronverters.

The results of this research will provide valuable insights into the transient stability of the German grid under different demand cases and disturbance scenarios. Furthermore, the study will highlight the effectiveness of grid-forming controllers in enhancing the system's stability. The findings will contribute to the ongoing efforts in optimizing grid operation and facilitating the integration of renewable energy sources within the German electricity network.

Contents

| | | |
|----------|--|-----------|
| 1 | Introduction | 1 |
| 2 | Theory | 2 |
| 2.1 | Network Reduction (Clustering) | 3 |
| 2.2 | ENTSO-E Grid Code | 4 |
| 2.3 | Maximum Demand Operation | 4 |
| 2.4 | Transient Stability of Power Systems | 5 |
| 2.5 | Stability Limit | 7 |
| 2.6 | Grid-Forming Controllers | 8 |
| 2.6.1 | Virtual Synchronous Machines | 9 |
| 2.6.2 | Synchronverter | 10 |
| 2.6.3 | Virtual Impedance | 12 |
| 2.7 | Control Models | 13 |
| 2.7.1 | Synchronous Machines Models | 13 |
| 2.7.2 | Inverter-Based Generators Models | 16 |
| 3 | Methodology | 19 |
| 3.1 | The Grid Model | 20 |
| 3.2 | Maximum Demand Case | 21 |
| 3.2.1 | Maximum Demand Including Loads Outside Germany | 24 |
| 3.2.2 | Maximum Demand Including Loads Only Inside Germany | 24 |
| 3.3 | Aggregation of Generators | 25 |
| 3.4 | Generation Dispatch | 30 |
| 3.4.1 | Generation Dispatch at Maximum Demand Considering Loads Outside Germany | 30 |
| 3.4.2 | Generation Dispatch at Maximum Demand Only Considering Loads Only Inside Germany | 31 |
| 3.5 | Study Cases & Scenarios | 34 |
| 4 | Results & Discussion | 37 |
| 4.1 | At Maximum Demand when Loads inside Germany only are Considered | 37 |
| 4.1.1 | Short Circuit at Synchronous Machine 40003 and Fault Clearance after 100 ms | 37 |
| 4.1.2 | Load Shedding | 41 |
| 4.1.3 | Using Synchronverters | 45 |
| 4.1.4 | Disconnecting Line 40000-40001, 100 ms after a Short Circuit Fault in the Middle of the Line | 47 |
| 4.2 | At Maximum Demand Considering Loads outside Germany | 49 |
| 4.2.1 | Disconnecting Synchronous Machine at Cluster 40003 | 49 |
| 4.2.2 | Load-Shedding | 52 |

| | | |
|----------|--|-----------|
| 4.2.3 | Disconnecting Line 40000-40001, 100 ms after a Short Circuit | |
| | Fault in the Middle of the Line | 55 |
| 4.3 | Comparison between the Two Maximum Demand Cases | 57 |
| 5 | Conclusion | 57 |

List of Figures

| | | |
|----|--|----|
| 1 | Synchronous generator connected to infinite bus [1] | 6 |
| 2 | VSM block diagram | 10 |
| 3 | Synchronverter block diagram | 11 |
| 4 | Synchronous Machine Composite Model | 13 |
| 5 | AVR block diagram | 14 |
| 6 | LFC block diagram | 14 |
| 7 | PSS block diagram | 15 |
| 8 | Composite Model Connections | 16 |
| 9 | Wind turbine composite model | 17 |
| 10 | Wind generator composite model connection | 17 |
| 11 | Solar generator composite model | 18 |
| 12 | Solar generator composite model connection | 18 |
| 13 | VSM composite model | 19 |
| 14 | VSM composite model connection | 20 |
| 15 | The reduced grid to be used in this research [2] | 21 |
| 16 | Density of clusters in the German Northwestern grid | 22 |
| 17 | Annual load curve at cluster 40006 [3] | 23 |
| 18 | Annual load curve at cluster 40007 [3] | 23 |
| 19 | Load flow at cluster 40000 at the max. demand inside Germany case | 30 |
| 20 | Generation dispatch in February 2020 [4] | 32 |
| 21 | Generation dispatch in January 2020 [5] | 32 |
| 22 | Location of cluster 40003 | 34 |
| 23 | Location of line 40000-40001 | 36 |
| 24 | Frequency response for case 4.1.1 | 38 |
| 25 | Voltage response for case 4.1.1 | 39 |
| 26 | Frequency response for case 4.1.1 with damper winding tuning | 39 |
| 27 | Voltage response for case 4.1.1 with damper winding tuning | 40 |
| 28 | Frequency response at 7% load shedding of total load | 42 |
| 29 | Voltage response at 7% load shedding of total load | 42 |
| 30 | Frequency response at 8% load shedding of total load | 43 |
| 31 | Voltage response at 8% load shedding of total load | 44 |
| 32 | Frequency response at 20.6% load shedding of total load | 44 |
| 33 | Voltage response at 20.6% load shedding of total load | 45 |
| 34 | Frequency response of VSM and synchronverter for 20.6% load-shedding | 46 |
| 35 | Frequency response for the case in 4.1.4 | 48 |
| 36 | Voltage response for the case in 4.1.4 | 48 |
| 37 | Frequency response for case 4.2.1 | 50 |
| 38 | Voltage response for case 4.2.1 | 51 |
| 39 | Frequency response at 9.26% load shedding of total load | 52 |
| 40 | Voltage response at 9.26% load shedding of total load | 53 |

| | | |
|----|--|----|
| 41 | Frequency response at 13.46% load shedding of total load | 54 |
| 42 | Voltage response at 13.46% load shedding of total load | 54 |
| 43 | Frequency response for case 4.2.3 | 56 |
| 44 | Voltage response for case 4.2.3 | 56 |

List of Tables

| | | |
|----|---|----|
| 1 | Loads values at maximum demand including interconnectors | 24 |
| 2 | Loads values at maximum demand only inside Germany | 25 |
| 3 | Generators per source at cluster 40000 to be aggregated | 26 |
| 4 | Aggregated solar generators at each cluster | 27 |
| 5 | Aggregated wind generators at each cluster | 28 |
| 6 | Aggregated conventional generators at each cluster | 29 |
| 7 | Dispatch at the maximum demand considering outside Germany . . . | 31 |
| 8 | Generation dispatch at maximum demand inside Germany | 33 |
| 9 | Results for disconnecting synchronous machine 40003 after a short-circuit | 40 |
| 10 | Results for 20.6% load-shedding of total load | 46 |
| 11 | Results for shorting and disconnecting line 40000-40001 | 49 |
| 12 | Results for case 4.2.1 | 51 |
| 13 | Results for 13.46% load-shedding of total load | 55 |
| 14 | Results for shorting and disconnecting line 40000-40001 | 57 |

Glossary

- AVR: Automatic-Voltage Regulator
- DSL: DIgSILENT Simulation Language
- ENTSO-E: European Network Transmission System Operators for Electricity
- GFC: Grid-Forming Controller
- LPF: Low-Pass Filter
- LFC: Load-Frequency Controller
- OS: Overshoot
- *PF*: Power Factor
- PID: Propotional-Integral-Differentiator
- PI: Proportional-Integral
- PLL: Phase-Locked Loop
- PSS: Power System Stabilizer
- ROCOF: Rate of Change of Frequency
- SCR: Short Circuit Ratio
- SI: Synthetic Inertia
- TSO: Transmission System Operator
- US: Undershoot
- VSM: Virtual Synchronous Machine
- VSC: Voltage-Source Converter
- WEC: Wind Energy Converter

1 Introduction

With the increasing integration of inverter-based resources and the growing complexity of the German grid, ensuring transient stability has become a significant concern for grid operators. Transient stability refers to the ability of a power system to maintain synchronism and acceptable voltage and frequency levels following large disturbances [1]. With the large recent integration of renewable energy sources, the total inertia of the system is decaying, which leads to transient stability problems in the grid. The inertia acts as an immediate physical response (inertial response) which comes from the moment of inertia of rotors of synchronous machines. However, in the future with the increasing penetration of renewable energy sources, it's expected to switch off more synchronous machines to decrease their carbon footprint which leads to the loss of their inertia. To address this challenge, grid-forming controllers, such as Virtual Synchronous Machines (VSMs) and synchronverters, have been proposed as potential solutions.

Virtual synchronous machines have the ability to copy the behaviour of synchronous machines in what's recently called injecting synthetic inertia (SI) into the power system [6]. Therefore, the importance of the role of this technology can be investigated to determine its feasibility when it comes to large disturbances like a severe short circuit fault at a generator's terminal. The transient stability which includes frequency response and voltage response will be studied then under the effect of this synthetic inertia. Several studies were made on the effect of emulating GFCs on transient stability such as "Study of virtual synchronous machine (VSM) converter controller response on frequency and transient stability" which is published in "2018 Conference on Power Engineering and Renewable Energy (ICPERE)". The study focuses on load-shedding and transmission line shorting and switching it out scenarios [7]. The study proves the effectiveness on VSMs for bringing the power system to stability after large disturbances. Also, the study "Virtual Synchronous Generator with Limited Current – Impact on System Transient Stability and Its Mitigation" published in "2020 IEEE Energy Conversion Congress and Exposition (ECCE)" studies the limited active power that can be emulated into the grid by VSMs and its impact on transient stability and how to mitigate this limitation on active power emulation [8]. However, the performance of the VSMs on the transient stability of actual grids is still under investigation. **The influence of SI on a system that works as the most important parameter in VSM was not analyzed [9].** Thus, this research will test in particular the influence of the SI on the transient stability of the German grid which is represented in more details in the Northwestern part when emulating VSMs and tune their parameters to fit in the grid.

The approach followed in this thesis is obtaining a model of the German grid that gives a good approximation when conducting transient stability studies, identify the maximum demand point and its corresponding time within Germany, and

explore scenarios that incorporate overall load including loaded interconnectors with neighbouring countries (external loads), and a restricted case when the demand only inside Germany is at its maximum value.

The aim of this thesis is to conduct a comparative transient stability study under various large disturbance cases on an actual grid [7] [1]. This comparative study compares the transient stability response of the German grid with deploying GFCs and the transient stability response of the same grid that is currently operating with its controllers. In other words, the knowledge gap that this research focuses on is the influence of the SI on transient stability in the actual German grid which is not investigated yet [9]. This analysis will be carried out using currently-used controllers in inverter-based resources (IBRs) and then using GFCs. In the literature, different GFCs can be used to mimic and emulate SI and the behaviour of synchronous machines like VSM. Another GFC in the literature is the synchronverter, where the main difference between them is using different modelling parameters like torque instead of power, and that is further discussed in the literature chapter [10][11]. This research will focus on the VSM approach because the main objective of this research is to compare the behaviour of VSM and currently-used controllers in inverter-based resources, and the time frame of this research is not enough to discuss both the VSM and the synchronverter in detail.

The theoretical section of this thesis will discuss the scientific principles underlying power system stability, synchronism, voltage regulators, load frequency controllers, power system stabilizers, and the mathematical representation and equation of VSMs and synchronverter. In the methodology section, the research approach employed in this study will be detailed, covering aspects such as grid modelling, parameter optimization, control strategy implementation, and simulation scenarios. Subsequently, the results and discussion section will present and analyze the obtained outcomes and accompanying graphs that illustrate the results. Finally, in the conclusion section, the findings of this research will be summarized, and recommendations will be provided based on the results obtained. Through this thesis, it is aimed to contribute to the ongoing development of grid-forming controllers by refining the design and parameters of VSMs and test their effect on the German grid. This research will aid in the advancement of reliable and resilient power systems. At the end, this research proves a better performance of transient stability especially for frequency response when emulating VSMs in the German grid.

2 Theory

This part implements the necessary theory that is used in this research. First, the network reduction (clustering) principle will be discussed briefly. Then, relevant details in the ENTSO-E grid code will be presented. Furthermore, power system

operation at maximum demand significance will be introduced. After that, the theory part will particularly revolve around transient stability. Finally, the theory behind grid forming controllers and the mathematical modelling will be represented thoroughly.

2.1 Network Reduction (Clustering)

Network reduction, also known as clustering, is a powerful technique employed in power systems to simplify complex grid structures while retaining essential characteristics. Network reduction offers a solution by condensing the representation of power systems while preserving their critical features [12]. The grid model used in this research is approximated using network reduction to give realistic results when conducting transient stability.

The main issue in carrying out this research is that the actual transmission grid which is used by the TSOs is not available. Hence, the grid was built based on an approximation of available calculations and measurements like power, voltage, and current.

However, the primary objective of network reduction is to reduce computational complexity while maintaining an acceptable level of accuracy. By clustering or grouping together nodes and branches based on their electrical proximity or similar characteristics, a reduced model is obtained. This condensed model captures the dominant behaviour and interconnections of the original system, enabling efficient analysis without compromising the overall system response.

One common method of network reduction involves the aggregation of buses or nodes. Buses with similar voltage magnitudes, phase angles, active power and reactive power load characteristics are combined into single representative buses. Generators are also combined as an equivalent voltage source with equivalent impedance which is known as Ward equivalent method in network reduction. This consolidation reduces the overall number of equations and variables in the system, resulting in faster simulation times. The aggregated buses retain the essential load-flow and stability characteristics of the original system. Other available network reduction techniques like particle swarm optimization (PSO) are also used.

In real-time operational studies, network reduction proves valuable in evaluating the transient stability of power systems. By reducing the system to its essential elements, engineers can perform stability analysis more expeditiously, enabling faster decision-making during critical grid events. This allows for proactive control and mitigation actions to maintain system stability and prevent cascading failures.

While network reduction offers significant advantages in terms of computational efficiency, it is essential to acknowledge that it introduces some approximation errors.

The reduced model may not capture all the nuances and interactions of the original system. Therefore, careful validation and sensitivity analysis is necessary to ensure the accuracy and reliability of the results obtained from the reduced model [12].

2.2 ENTSO-E Grid Code

The ENTSO-E Grid Code serves as a comprehensive framework for the operation and development of Europe's electricity transmission system. It outlines the technical and operational requirements that ensure the reliable and efficient functioning of the grid. From voltage levels and power quality to interconnection standards, this code establishes guidelines for grid operators and stakeholders to maintain stability and facilitate cross-border electricity flows[13].

From the ENTSO-E Grid Code, it is stated that the nominal frequency is 50 Hz, the standard frequency range deviation is 50 mHz, the maximum steady-state frequency deviation is 200 mHz, and the maximum instantaneous frequency deviation is 800 mHz [14]. If the frequency range is 49.0 Hz - 51.0 Hz, synchronous generators have to be able to stay connected to the grid for an unlimited time. Regarding the RoCoF, the power-generating modules shall remain stable and connected to the grid as follows: 500 ms for a RoCoF absolute value of 2 Hz/s, 1000 ms for 1.5 Hz/s, and 2000 ms for 1.25 Hz/s [15]. Regarding the voltage range, for connection points between 110 kV and 300 kV is 0.9 pu - 1.1118 pu. For connection points between 300 kV and 400 kV, the voltage range is 0.9 pu - 1.05 pu [14].

2.3 Maximum Demand Operation

The effect of maximum grid demand on the stability of the power grid is a crucial consideration for power system operators and planners. While transient stability refers to the ability of the power system to maintain synchronism and recover stable operation following severe disturbances, such as faults or sudden changes in load or generation. Maximum grid demand can contribute to transient stability challenges. During peak demand periods, the system may operate closer to its stability limits, leaving less margin for responding to disturbances. sudden changes are more likely to happen during peak periods which can lead to exceeding the system's transient stability limits, leading to voltage instability, oscillations, or even cascading failures [16]. Proper analysis and control of transient stability during high-demand scenarios are crucial for maintaining the grid's stability because in large disturbances, parameters have to be tuned perfectly, and the right choice of controllers and their time delay and proper operation can affect the frequency and voltage response and how do they respond to large disturbances. TSOs use different cases to test for the stability of the grid like short circuiting generators and disconnecting them afterwards and observe the behavior of the response of the system [17].

Maximum grid demand significantly affects the stability of the power grid, including steady-state stability, transient stability, and reserve capacity requirements. Proper management of peak demand through accurate forecasting, load management strategies, and sufficient generation capacity is crucial for maintaining a stable and reliable power system. By effectively addressing the stability challenges associated with high-demand periods, power system operators can ensure a continuous and secure supply of electricity to consumers.

2.4 Transient Stability of Power Systems

Traditional stability analysis in power systems includes frequency stability, voltage stability, and rotor angle stability. What is meant by stability is keeping the values of voltage and frequency within the tolerable limits and that depends on the grid code of the country or region [1]. Synchronism is keeping operating at the nominal frequency under different conditions whether they are a slight or large disturbance in power systems without harmful oscillations between different generators that can affect normal load flow conditions or initiate protection elements that might isolate some components. A power system operates at synchronism if the whole system is operating at the nominal frequency (i.e. 50 Hz) in Germany. The position of the speed of the rotor angle determines the frequency of the power system. The rotor angle (also known as the power angle, or torque angle) is defined in many ways. From a power systems perspective, it is the voltage angle difference between the sending end and the receiving end in the power system [1]. The equations that implement the relationship between the two types of power (active and reactive) and the rotor angle are as follows [18]:

$$P = \frac{3 V_t V_o}{X_t} \sin\delta \quad (1)$$

$$Q = \frac{3 V_o (V_o \cos\delta - V_t)}{X_t} \quad (2)$$

Where P and Q are the active and reactive power, respectively. V_t is the magnitude of the voltage at the sending end, and V_o is the voltage magnitude at the receiving end. X_t is the reactance in between and δ is the rotor angle. The flow of power can be seen in Fig 1.

Using this power angle as introduced in the previous equations, the active power flow can be controlled, and it also affects reactive power. The reactive power flow can be controlled by changing also the magnitude of the voltage at the sending end or the receiving end. Consequently, the power factor will change. Therefore, it can be seen how significant is the power angle, where all values are somewhat linked to it.

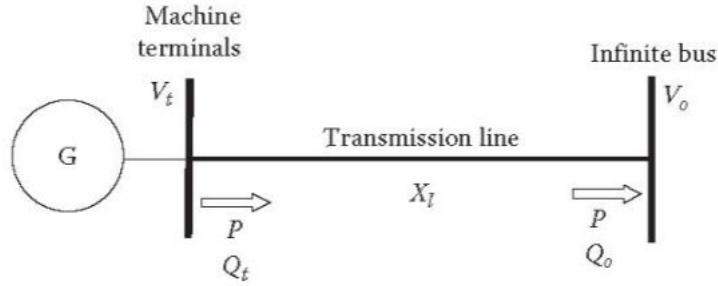


Figure 1: Synchronous generator connected to infinite bus [1]

However, if the rotor angle gained acceleration this would increase the speed of the angle and therefore increase the frequency. By the same measure, if a deceleration occurs, the frequency will decrease. This acceleration or deceleration happens due to the mismatch between the input power and the output power which is implemented by the electrical power of the power system. If the input power is higher than the output power, acceleration will happen. The mismatch can happen due to a sudden outage of a power plant or a sudden load shedding or other disturbances. The equation that governs the relationship between the power and rotor angle in synchronous machines is called the swing equation and it is shown below [18].

$$\frac{H}{\pi f} \frac{d^2\delta}{dt^2} = P_m - P_e \quad (3)$$

Where f is the synchronous frequency in Hz , δ is the rotor angle position, and $\frac{d^2\delta}{dt^2}$ represents the second derivative of the rotor's angle position which is the acceleration. In the steady-state operation, the term $\frac{d^2\delta}{dt^2}$ must equal 0, which means the rotor does not accelerate and therefore its speed $\frac{d\delta}{dt}$ is constant. The speed of the rotor angle represents the frequency of the grid, P_m and P_e are the mechanical (input) power and the electrical (output) power, and H is the inertia constant. In other words, when the demand P_e matches the input power P_m , the term $P_m - P_e$ is equal to 0. Therefore, the acceleration of the rotor is 0, and the speed of the rotor is constant which means the frequency is kept constant. Hence, the transient stability of frequency can be studied by investigating the speed of the rotor which is represented in the swing equation by the first derivative of the rotor's angle.

The inertia constant H is an important factor in the stability of power systems and it depends on the moment of inertia of the rotor, it is measured in seconds and it expresses the period that the synchronous machine will be able to provide its rated power when a large disturbance occurs and this is the physical inertial response that kicks in immediately when a disturbance happens [18]. This inertial response is actually what non-conventional generators like renewable energy sources lack because in the case of solar generators there is no rotating mass, and there is no

moment of inertia at all. In the case of wind turbines, the rotor mass and moment of inertia are much smaller than in the rotating masses of synchronous machines. The inertia constant can be expressed as in the following equation.

$$H = \frac{E_r}{S} \quad (4)$$

Where E_r is the mechanical energy stored in the rotor measured in MJ, and S is the rated apparent power of the synchronous machine measured in MVA, thus H is measured in seconds.

After the wide penetration of renewable energy sources and the use of power electronic converters like voltage source converters (VSCs) and line commutating converters (LCCs), a new term of stability showed up which is converter-based stability. The non-linear devices can cause harmonics, resonance, and converter-driven stability. Inverter-based resources have low short circuit ratio (SCR) which weakens the grid resulting in a weak grid. A weak grid is a grid that has high short circuit impedance or low short circuit ratio [19]. This results into variations in voltage and frequency in case of small changes in the current or power, and it's hard to maintain the stability of the grid in case of low SCR. That's why grid-forming converters kick-in where they are able to form the voltage autonomously from the grid conditions and therefore support weak grids [6]. For the future, employment of VSM as grid forming controllers is also one step ahead to compensate for the lack of inertia. In the literature, it is common to study the effect of VSM on power systems by testing them for sudden disturbances like short circuit faults and faults clearance, and load shedding for example: 5% shedding of the load [7]. In Europe, TSOs perform standard test cases like system splits and their impact on the RoCoF. One example is global severe splits which focuses on split scenarios that results in a $|RoCoF|$ that exceeds 1 Hz/s in a subsystem [17].

Large disturbances in power systems are defined in four cases [1]:

1. Severe three-phase fault at the sending end.
2. Sudden load change.
3. Three-phase fault at the transmission between the two voltage ends.
4. Switching out One of two-parallel transmission lines between the two voltage ends.

2.5 Stability Limit

In power systems, stability limit refers to the maximum power transfer capability of a system without causing instability or voltage collapse or damage in equipment.

It represents the boundary beyond which the system cannot sustain stable operation. When the power transfer, frequency, or voltage exceed this limit, the system may experience voltage fluctuations, oscillations, or even a complete blackout, and equipment life shortening or even damage.

What actually of an importance in this research is the large stability limit which is studied using various terms, including:

1. Rotor angle limit: From equation 1, it can be seen that to achieve a maximum power transfer, δ has to equal $\pi/2$. So, when the angle δ oscillates after a large disturbance its final state has to be less than or equal to $\pi/2$. If the rotor angle exceeds its stability limit, that means the acceleration of the rotor will keep increasing. This will result into damaging problems, such as generators disconnection and losing the supply of the system, because if the rotor keeps accelerating it will suffer from life-shortening or even damage [1].
2. Voltage stability: voltage stability is crucial since it is important in voltage synchronism between generators. Since stability of voltage is defined by its frequency, magnitude, and phase angle, if the voltage at a bus violates its stability limit it will lead to a loss of synchronism and therefore outages, because large violation in voltage results into a change in the value of magnetic flux of equipment such as transformers which requires large excitation current and therefore it can cause a serious damage in the transformer [1].

2.6 Grid-Forming Controllers

Unlike widely-spread grid-following converters, grid-forming converters can form voltage without commutation from the grid. They autonomously create voltage waveforms without following the grid [20].

Grid-forming controllers are advanced controllers for grid-forming converters that have been introduced to enhance the stability of power systems with a large share of non-conventional (renewable) generators that are interfaced via power electronic converters.

Power electronic converters act similarly to a controlled current source. This current source act can cause stability issues in weak grids which are grids with low short circuit ratio (SCR) that have a large impedance that might cause high voltage drop or grids with a high penetration of power electronic interfaced generators. Grid-forming controllers inject voltage source behaviour with inertia to overcome the issues of stability, especially in large disturbances.

In this research, two common types of grid-forming controllers will be employed and discussed:

1. Virtual synchronous machines
2. Synchronverter

Grid-forming controllers can also be used in combination with a virtual impedance which improves the damping which can replace the function of the damper winding in synchronous machines and allows for current limiting in the event of short-circuits [21][22].

2.6.1 Virtual Synchronous Machines

A VSM model can be represented using the behaviour of the synchronous machine which originally comes from the swing equation. The equation that will be applied to the VSM in the Laplace domain is [11]:

$$T_a s w = p_{set} - p_{mea} - D_p (w_r - w_{set}) \quad (5)$$

where T_a is the mechanical time constant, p_{set} is the active power set point and p_{mea} is the measured active power output. The rotating speed of the VSM is given by w_r , w_{set} is the frequency set point and D_p is the damping coefficient. Furthermore, in addition to the swing equation, a low-pass filter ($\frac{w_c}{w_c + w_s}$) is applied in the damping part. This allows for inertia injection during transient disturbances, while eliminating the impact of the damping term at steady-state, i.e. eliminating the droop.

The block diagram of the VSM is shown in Figure 2 [11]. Where f_{nom} is the nominal frequency, f_{ref} is the reference frequency in RMS simulation, and θ_v is the output voltage angle.

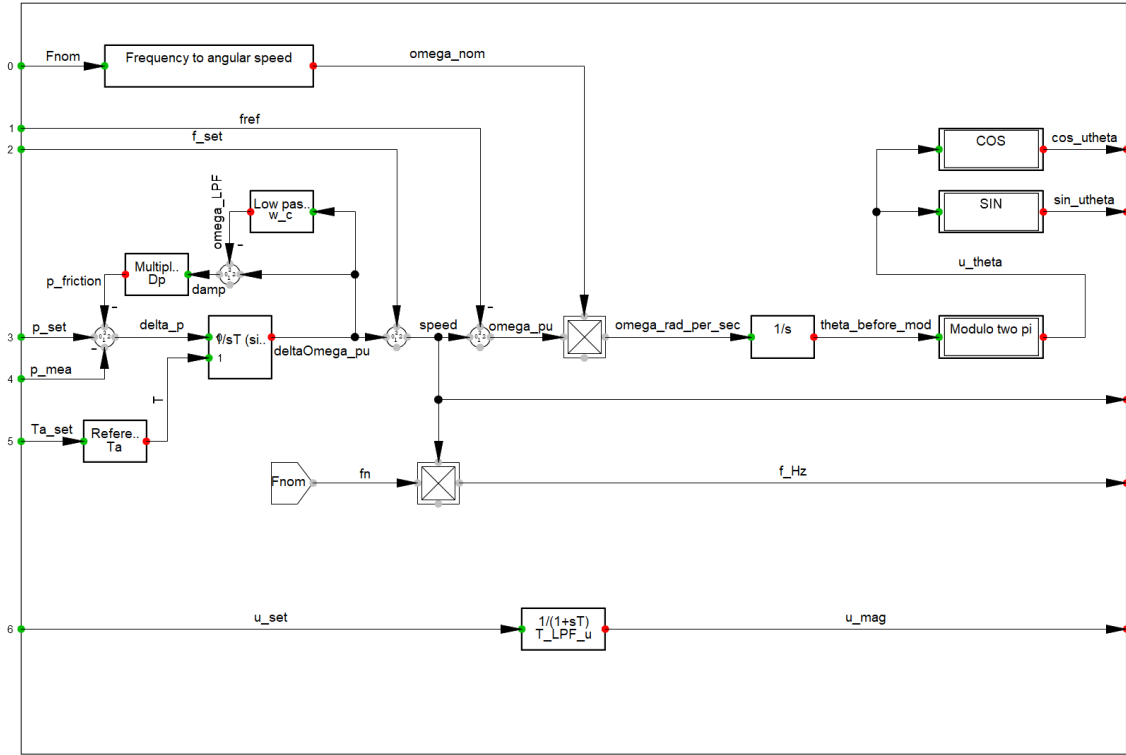


Figure 2: VSM block diagram

p_{mea} can be calculated using the equation below [11]:

$$p_{mea} = u_r i_r + u_i i_i \quad (6)$$

where u_r and u_i are respectively the real and imaginary parts of the output voltage, i_r and i_i are the real and imaginary currents of the output current, respectively.

2.6.2 Synchronverter

The Synchronverter controller is also based on the swing equation and similar to the VSM, except that the torques t_{set} and t_{calc} are used instead of p_{set} and p_{mea} . The main differences to the VSM are the additional reactive power control and the controller output voltage being used for the power-torque calculation instead of the measured voltage [10].

The synchronverter block diagram is shown in Figure 3 The parameters above can be calculated using the following equations [10]:

$$t_{calc} = M_f i_f (i_{a,mea} \sin(\theta_r) + i_{b,mea} \sin(\theta_r - \frac{2\pi}{3}) + i_{c,mea} \sin(\theta_r - \frac{4\pi}{3})) \quad (7)$$

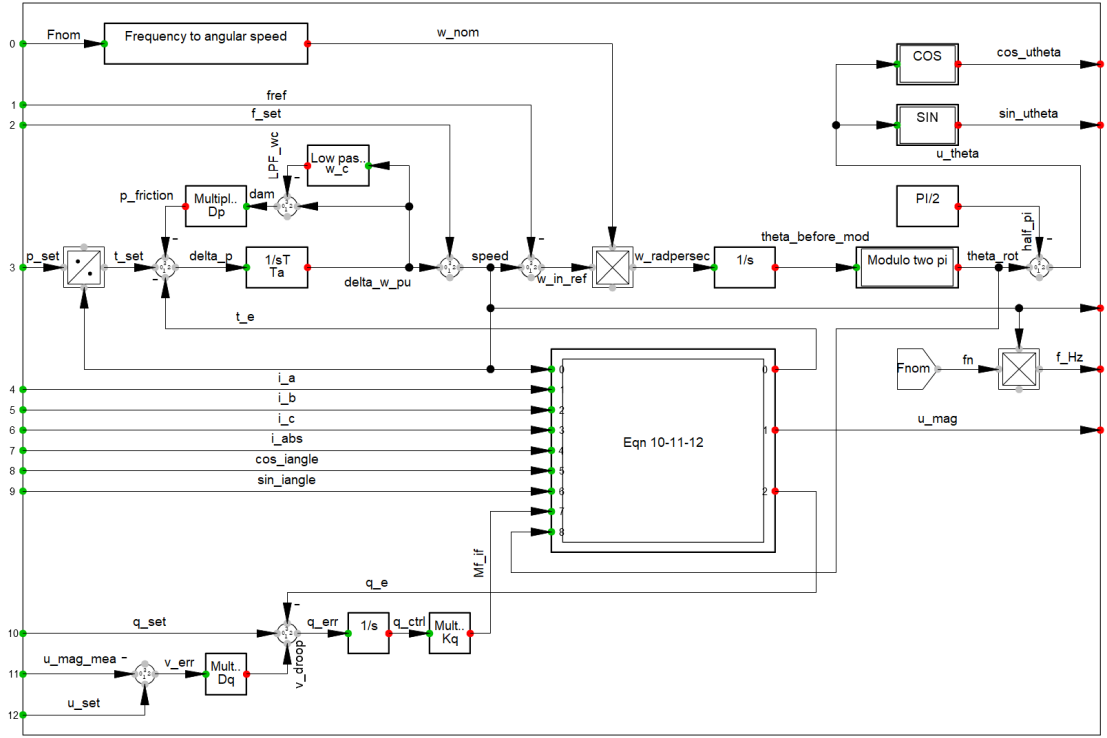


Figure 3: Synchronverter block diagram

$$q_{calc} = \dot{\theta}_r M_f i_f (i_{a,mea} \cos(\theta_r) + i_{b,mea} \cos(\theta_r - \frac{2\pi}{3}) + i_{c,mea} \cos(\theta_r - \frac{4\pi}{3})) \quad (8)$$

$$u_{s,mag} = \dot{\theta}_r M_f i_f \quad (9)$$

The excitation current source is denoted as $M_f i_f$, where M_f stands for the main field and i_f represents the field current. The $M_f i_f$ term represents the main excitation control loop, which adjusts the field current to regulate the generator's terminal voltage.

By controlling the excitation current, the simplified excitation model in the VSM allows for voltage regulation and helps maintain system stability during normal and transient operating conditions. $i_{abc,mea}$ is the measured output current and θ_r is the rotor angle. The reactive power controller consists of an integral controller with the gain K_1 . The reactive power error q_{err} depends on the set value q_{set} , the calculated value q_{calc} and the voltage droop as follows [10]:

$$q_{err} = q_{set} q_{calc} D_q (u_{mag,mea} u_{set}) \quad (10)$$

where $u_{mag,mea}$ is the measured voltage magnitude, u_{set} is the the voltage set point and D_q is the voltage droop coefficient. The stator voltage θ_u is proportional to the

change of flux induced by the rotor field and, therefore, lags the rotor angle θ_r by $\pi/2$.

The frequency Δw_{droop} and voltage magnitude Δu_{droop} deviations from the load flow initialization are calculated according to the following equations [21]:

$$\Delta w_{droop} = m_p \Delta p_{LPF} \quad (11)$$

$$\Delta u_{droop} = m_q \Delta q_{LPF} \quad (12)$$

where m_p and m_q are the active and reactive power droop coefficients and Δp_{LPF} and Δq_{LPF} are the low-pass filtered active and reactive power deviations from the load flow initialization, respectively. The parameters f_{set} , p_{set} , u_{set} and q_{set} are usually initialized according to the initial load flow. However, they are modelled as input variables to the droop controller and, therefore, can be controlled from outside the block.

2.6.3 Virtual Impedance

Virtual impedance is used as a damper in the virtual synchronous machine which plays the same role as the damper winding in the synchronous machine in transient or large disturbances. In combination with the VSM or synchronverter it achieves both the immediate physical inertial response and the damping functions of the synchronous machine.

The real and reactive voltage drop over an algebraic type virtual impedance is calculated as follows [21]:

$$\Delta u_{vi,r} = r_{vi} i_{vi} - x_{vi} i_{vi,i} \quad (13)$$

$$\Delta u_{vi,i} = r_{vi} i_{vi} + x_{vi} i_{vi,r} \quad (14)$$

where r_{vi} is the resistance constant (i.e. 0.06 pu in this case) and x_{vi} is the reactance constant (i.e. 0.06 pu) of the virtual impedance [21]. The current i_{vi} is the current supplied by the converter. The virtual impedance controller is used to change the impedance parameters according to grid conditions. The virtual impedance increases during short circuit events for example to limit the short circuit current. The virtual impedance is adjusted in proportion to the low-pass filtered current absolute value $|i_{vi}|$ when a certain threshold i_{lim} is exceeded as given in [22]:

$$z_{vi} = \begin{cases} r_{vi} + jx_{vi} & \text{if } |i_{vi}| \leq i_{lim} \\ (k_{pr} r_{vi} + jk_{px} x_{vi})(|i_{vi}| - i_{lim}) + r_{vi} + jx_{vi} & \text{if otherwise,} \end{cases}$$

where k_{pr} and k_{px} are the proportional factors constants for the virtual resistor and virtual reactance, respectively.

2.7 Control Models

In transient stability, dynamic models for generation units play a vital role. In this section, dynamic and control models of synchronous machines, and inverter-based resources that are used in this research will be discussed.

2.7.1 Synchronous Machines Models

For synchronous machines, the whole control model (composite model) consists of three main controllers, LFC, AVR, and PSS. These controllers and their parameters will be briefly discussed in this research and not thoroughly because it is more relevant to the linear control theory.

Figure 4 shows a brief of the composite model used in synchronous machines. These three basic controllers will be able to maintain the basic function of stability during large disturbances [1].

| | Slots BlkSlot | Net Elements Elm*,Sta*,IntRef,IntVecobj |
|---|------------------|--|
| 1 | Sym Slot | ✓  Synchronous Machine |
| 2 | Avr Slot | ✓  AVR |
| 3 | Gov Slot | ✓  LFC |
| 4 | Pss Slot | ✓  PSS |

Figure 4: Synchronous Machine Composite Model

Each Synchronous machine at each cluster will have a composite model with its controllers like the above. For simplicity, these controllers and their constants were represented as mentioned in the textbook Power System Analysis by Hadi Saadat, built using Simulink and used in PowerFactory. Figures 5,6 and 7 show the block diagrams of the basic AVR, LFC, and PSS, respectively that are used in this research [1]. The connection between the controllers is shown in Figure 8.

The AVR controllers is used to regulate the terminal voltage at the infinite bus of the generator. Its general principle of operation is to have negative feedback from the actual voltage value and compare it with the reference value which will result in the error value. Then, the excitation (field current) of the synchronous machine will be adjusted in a way that produces flux to keep the voltage value within tolerable limits [1]. As can be seen in the graph, the input values of the controller are voltage values. Then, they will be processed and compared and other blocks might be applied such as LPF or voltage limiters might be applied. The most important part is the PID controller which keeps fixing, adjusting, and expecting the error in the voltage value continuously. In this research, the details of these controllers will not be thoroughly investigated since they are more relevant to the control theory.

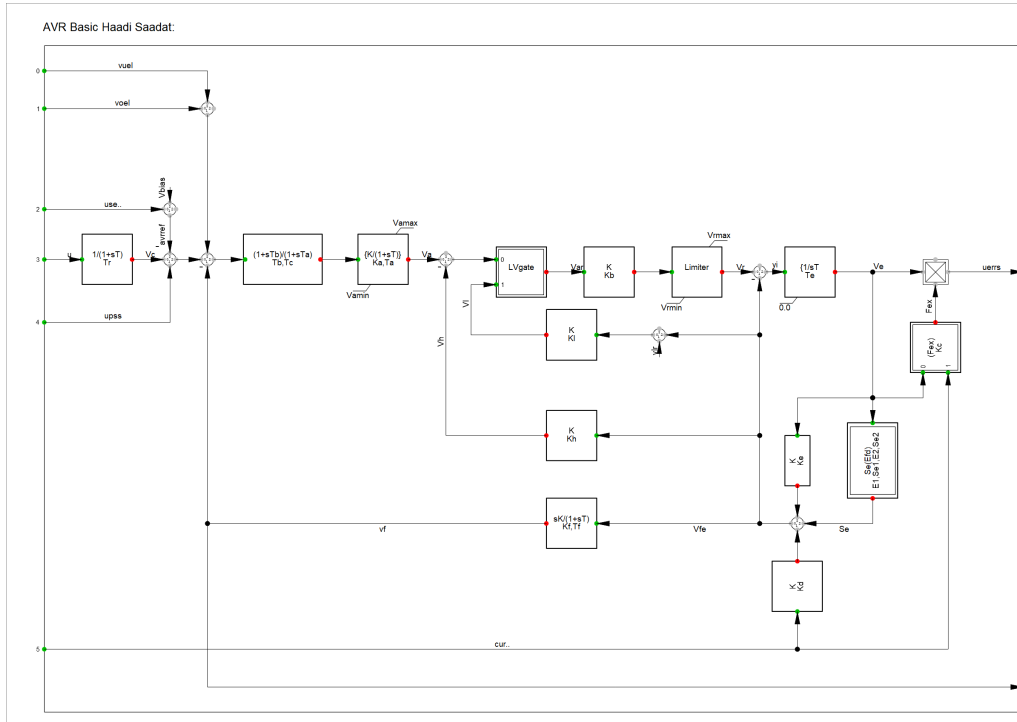


Figure 5: AVR block diagram

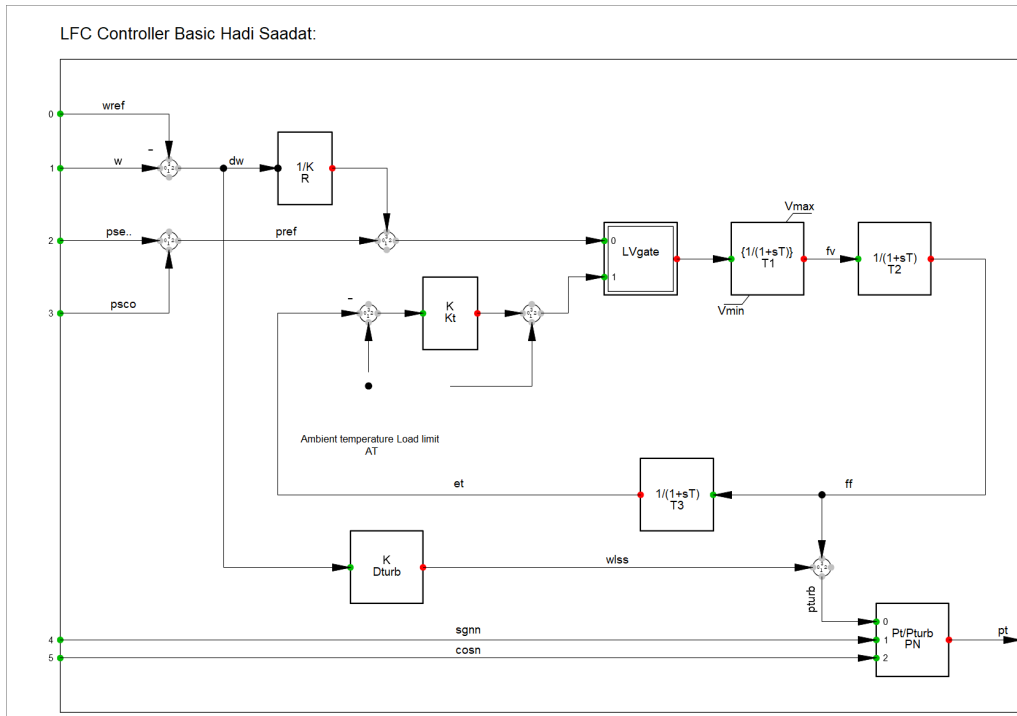


Figure 6: LFC block diagram

The LFC controllers are controllers that maintain the frequency value of the synchronous machine within tolerable limits. This is done by measuring the output power of the generator continuously and comparing it with the set point of the controller, then the resulting error will pass through a PID controller. The significance of PID controllers is that the P (proportional) part compensates for big instantaneous errors, while the I (integral) part integrates the error over time and compensates for its accumulated value. Finally, the D (derivative) part finds the slope of the error pattern and therefore can expect the future value of the error and compensate for it. The resulting adjustment will be given as an order to the governor to provide more or less mechanical power. The input parameters of the LFC controllers are the set points of frequency and power, and the actual values of them as well [1].

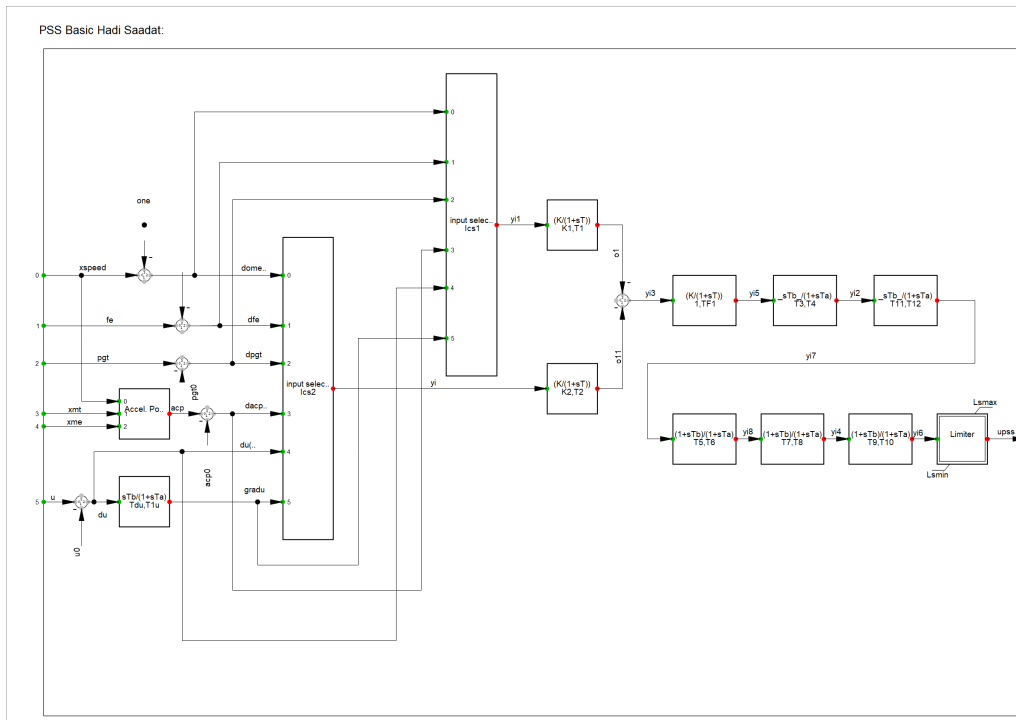


Figure 7: PSS block diagram

The power system stabilizer improves the system's transient and dynamic response, reducing the risk of instability and kicking in immediately with a big proportional constant that lifts the system up in the case of a large disturbance [23]. The main function of a power system stabilizer is to dampen frequency oscillations in the electrical power system. The input parameters of the PSS are voltage and frequency together with many cascaded controllers and limiters.

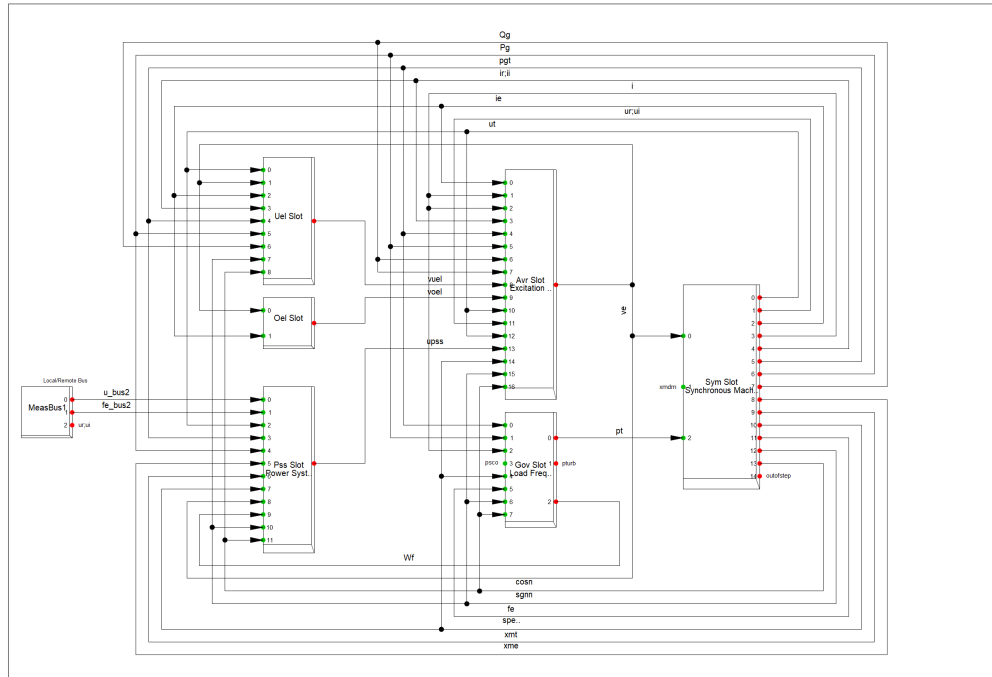


Figure 8: Composite Model Connections

2.7.2 Inverter-Based Generators Models

The inverter-based resources control is of significant importance in the grid, because they adjust the behaviour of renewable energy sources to maintain the stability of the grid since the nature of these renewable sources is fluctuating and is not fixed. Currently-used controllers will be shown and then GFCs that are under development will be discussed as well.

A composite model of the currently-used control strategies of wind turbines is shown in Figure 9. The connection between the dynamic models is shown in Figure 10.

It can be seen that the composite model consists of many mechanical and electrical controllers like the pitch angle control model, aerodynamic control model, torque control model, and others [24]. Similarly, The solar generator composite model is shown in Figure 11 which consists of dynamic controllers, frequency controllers, PLL and others. The PLL makes sure the voltage angle of the output voltage of the solar generator follows the phase angle of the grid's voltage. These are the commonly used controllers now for inverter-based-resources [24]. The connection of the solar composite model is show in Figure 12.

| | Slots BlkSlot | Net Elements Elm*,Sta*,IntRef,IntVecobj |
|-----|-------------------|--|
| ▶ 1 | WT | ✓ Static Generator- Wind 40003 |
| 2 | Speed Ref | ✓ Speed Ref |
| 3 | Torque Control | ✓ Torque Control Model |
| 4 | Pitch Control | ✓ Pitch Model |
| 5 | AeroDynamic | ✓ Aero.Dyn Model |
| 6 | Drive-Train | ✓ Drive-Train Model |
| 7 | PQ Control | ✓ Electrical Control Model |
| 8 | Power Measurement | ✓ PQ Measurement T3 |

Figure 9: Wind turbine composite model

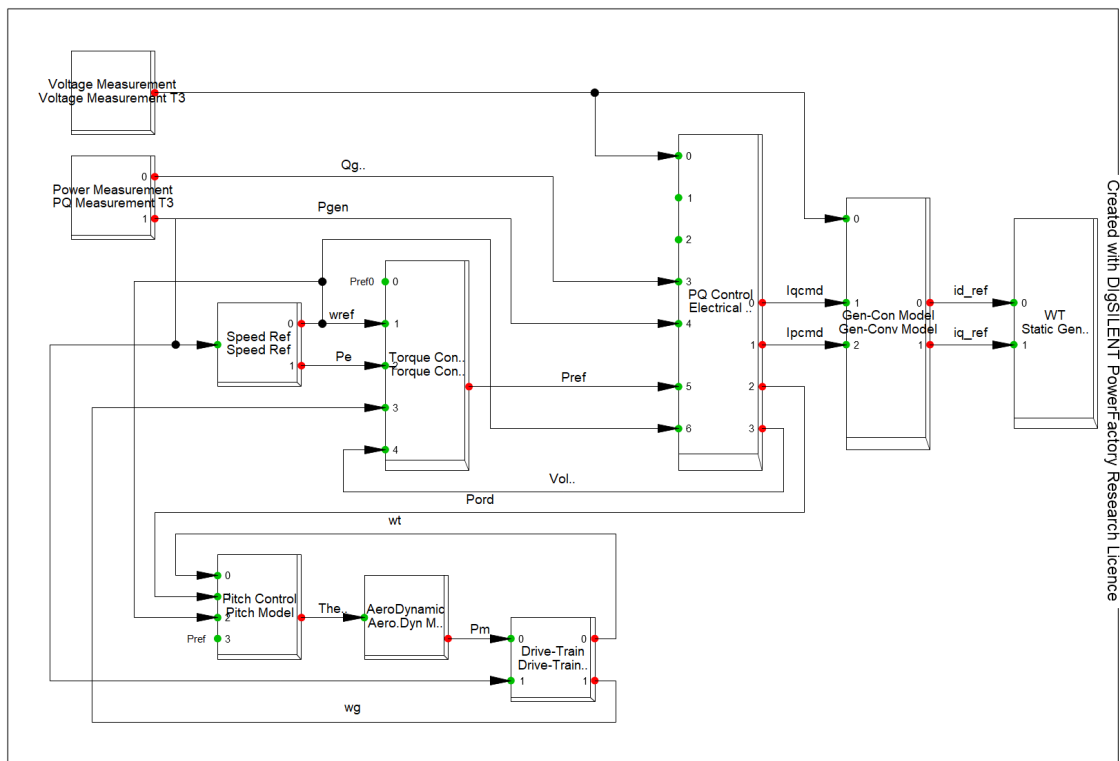
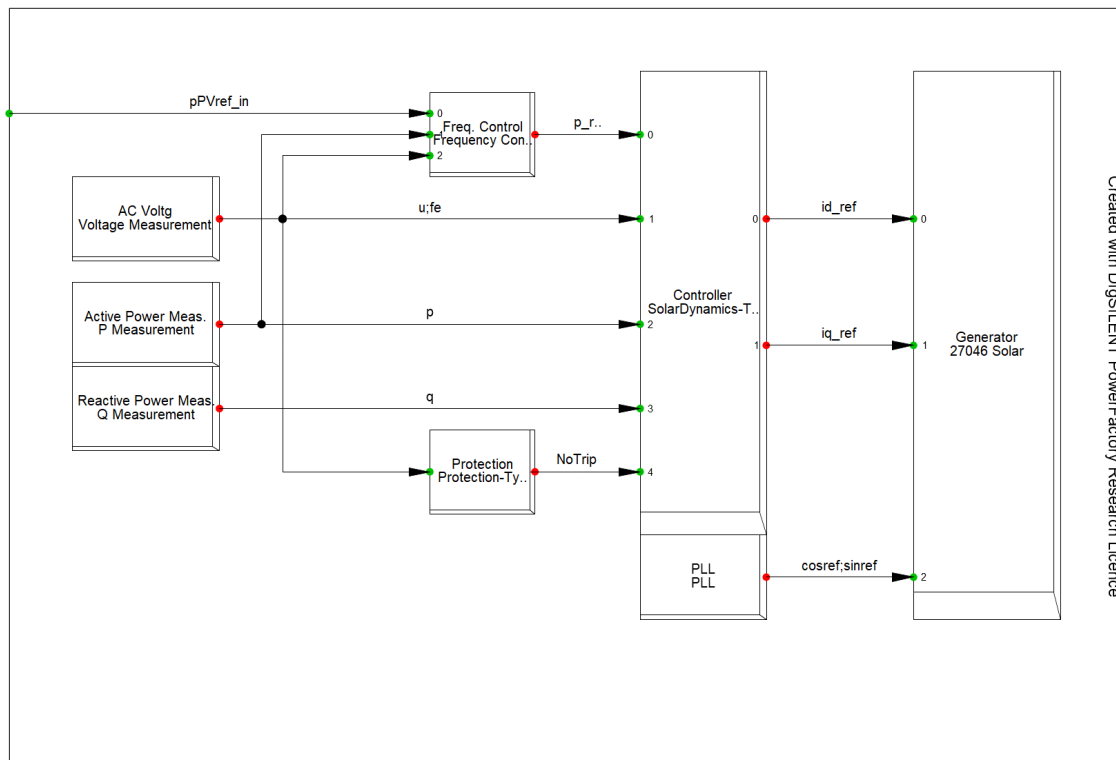


Figure 10: Wind generator composite model connection

| | Slots BlkSlot | Net Elements Elm*,Sta*,IntRef,IntVecobj |
|---|----------------------|--|
| 1 | Generator | ✓ 40003_a(1)_solar |
| 2 | Controller | ✓ SolarDynamics-Type C |
| 3 | Freq. Control | ✓ Frequency Control-Type C |
| 4 | Protection | ✓ Protection-Type C |
| 5 | PLL | ✓ PLL |
| 6 | AC Voltg | ✓ Voltage Measurement |
| 7 | Active Power Meas. | ✓ P Measurement |
| 8 | Reactive Power Meas. | ✓ Q Measurement |

Figure 11: Solar generator composite model



Created with DIGILENT PowerFactory Research Licence

Figure 12: Solar generator composite model connection

The VSM composite model can be shown in Figure 13. It can be seen that the composite model contains the VSM dynamic model itself which was shown and discussed in this chapter. Also, dynamic models play a supportive role like the virtual impedance in case of short circuit faults by controlling the impedance value to limit the short circuit current. As a composite model, it's expected also to have a voltage controller which is a PI controller in this case. It can be replaced by any more advanced voltage controller. However, the main objective of a VSM is to inject SI into the system to compensate for the absence of the physical inertial response. The connection of the composite model is shown in Figure 14.









| | Slots BlkSlot | Net Elements Elm*,Sta*,IntRef,IntVecobj |
|---|----------------------------|--|
| 1 | Converter | ✓  Static Generator- Wind 40003 |
| 2 | Grid-forming control | ✓  Virtual Synchronous Machine |
| 3 | Virtual impedance | ✓  Virtual Impedance |
| 4 | Voltage control | -  PI Voltage Controller |
| 5 | Power calculation | ✓  Power Calculation |
| 6 | Output voltage calculation | ✓  Output Voltage Calculation |
| 7 | Voltage measurement | ✓  Voltage Measurement |
| 8 | Current measurement | ✓  Current Measurement |

Figure 13: VSM composite model

3 Methodology

In this section, the information required and the raw data used in the research will be presented and the methods followed will be thoroughly discussed. It will start with the grid model used in this research. Then, the maximum load points inside and outside Germany will be determined because they are the most critical points. A Python code will be used to determine the values of maximum loads and their time, then this code will return the load value of each cluster at that time. The process of aggregating generators of different technologies considering their inertia constant H will also be illustrated. Then, the generation dispatch will be determined at the points of maximum demand based on open sources [3].

After that, different dynamic models for synchronous machines will be built using Matlab/Simulink based on textbooks in their basic forms. Also, dynamic models of wind and solar generators will be used where some of them are already existing and

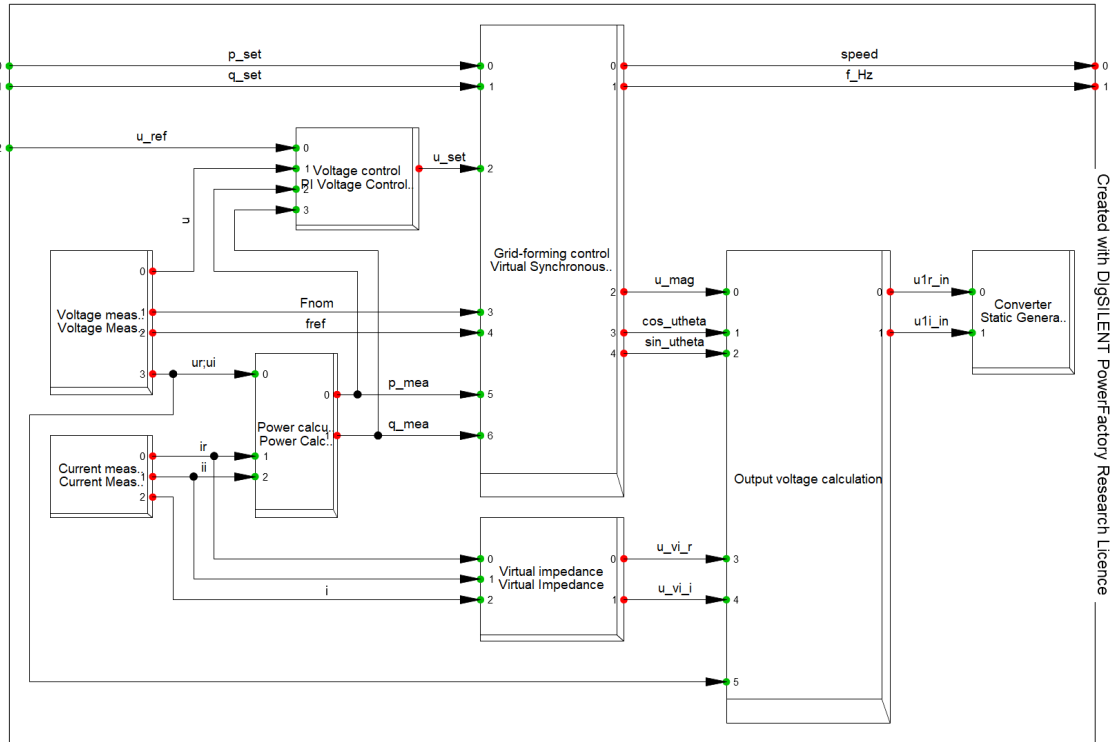


Figure 14: VSM composite model connection

some will be taken from the literature. Finally, grid-forming controllers' dynamic models will be used from the literature to start the simulation and compare the results.

3.1 The Grid Model

The data used in this research contains geographic information on the grid elements like transmission lines, transformers, nodes, generators and loads. In addition to this, electric parameters of these grid elements like voltage levels, transmission lines' length, lines impedances, and machines ratings are available [3]. These parameters and elements are used as input for the power grid modelling in PowerFactory [25]. The active and reactive power flows were calculated using AC load flow grid models which are part of the H2-ReNoWe project [2]. The used grid model in this research consists of 21 clusters and it is shown again in Figure 15.

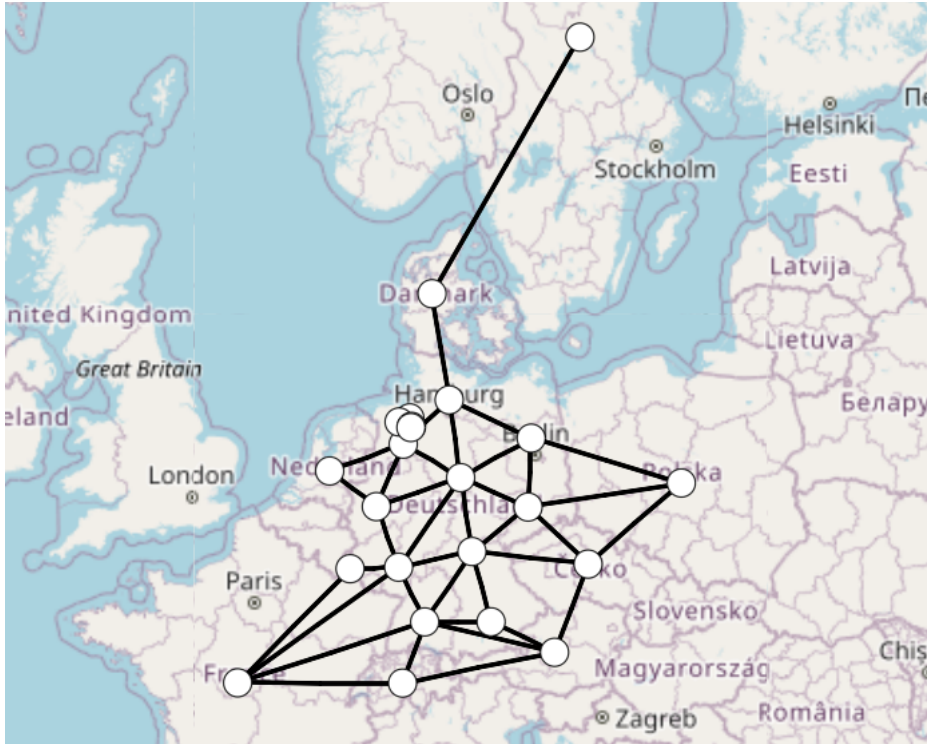


Figure 15: The reduced grid to be used in this research [2]

As mentioned before, the grid is represented in more detail in the Northwestern region. It is reduced in a way that does not affect the results of transient stability analysis. To simplify the study, each cluster will consist of one conventional generator, one solar PV generator, and one wind generator, and that is apart from the other components like transmission lines, loads, and transformers' impedance. The higher concentration and more accurate clusters in the German Northwestern grid can be seen in Figure 16.

More essential parameters were taken into consideration when building the grid model. Transformers were implemented using the transformer's impedance component. Synchronous generators depended on more parameters such as inertia constant, damping factor, generation dispatch, positive sequence direct-axis reactance, local controllers, and dynamic models. IBRs were implemented using their generation dispatch, local controllers, and dynamic models.

3.2 Maximum Demand Case

As mentioned in section 2.2, During peak demand periods, the system may operate closer to its stability limits, leaving less margin for responding to disturbances. Any large and rapid changes in demand or generation during peak periods can potentially exceed the system's transient stability limits, leading to voltage instability,

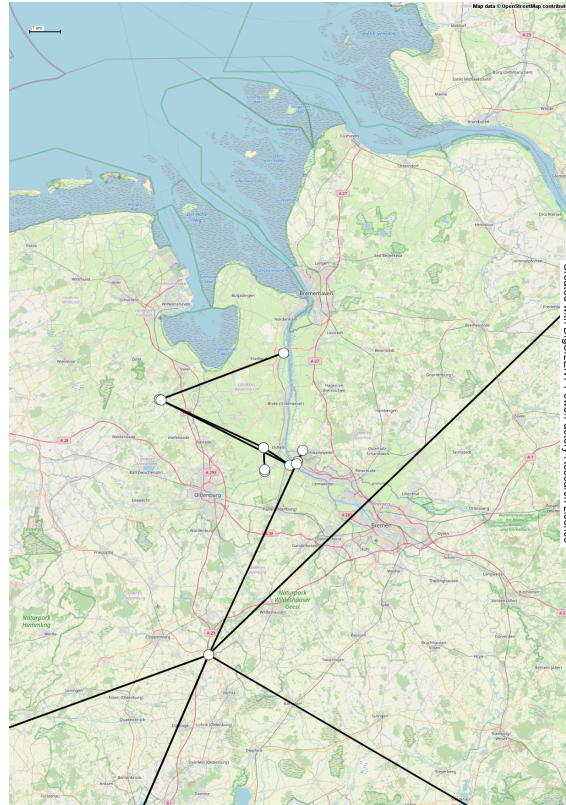


Figure 16: Density of clusters in the German Northwestern grid

oscillations, or even cascading failures. That's why it is important to study the transient stability of the system at the peak demand operation. As the German grid is connected to other neighbouring countries via interconnectors, these interconnectors can consume power acting as loads. Thus, the maximum demand shall include the power flow through the interconnectors. For further analysis and to consider more than one scenario, the time step when the maximum demand inside Germany occurs is also considered.

The maximum demand time steps are determined using the annual power consumption of loads taken from open-access grid data from the open_eGo project [3]. The data analysis was done using Python scripts which will be used to determine these points and their exact time of occurrence. Then, this will also return the value of each load at that moment.

The data of each cluster is provided as raw data by open_eGo project source. For example, Figure 17 below shows the annual profile of the load connected to cluster 40006.

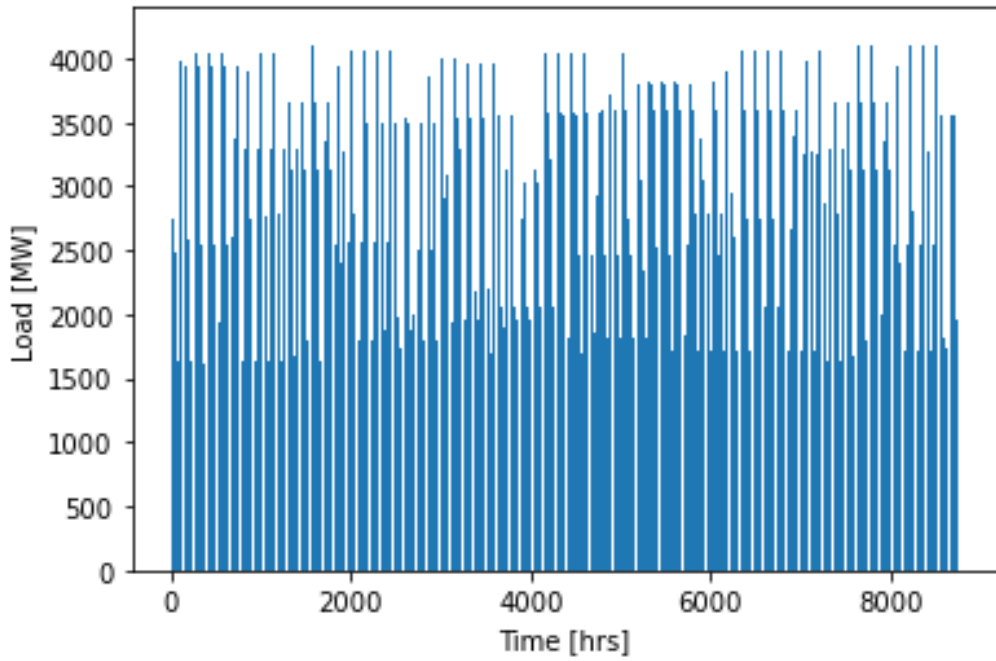


Figure 17: Annual load curve at cluster 40006 [3]

Similarly, the load profile of cluster 40007 can be shown in the Figure 18.

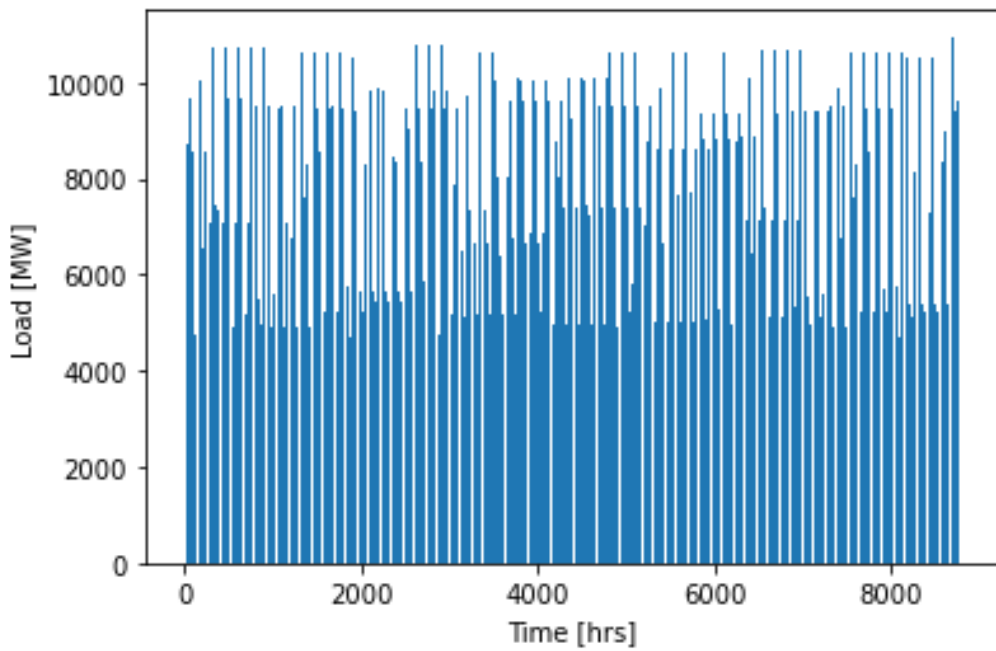


Figure 18: Annual load curve at cluster 40007 [3]

3.2.1 Maximum Demand Including Loads Outside Germany

After performing data analysis using Python, the maximum load including loads outside Germany (interconnectors) occurs in 2020 at hour number 1212 which will be Wednesday, 19 February 2020 at 13:00. The value of this maximum demand for the whole grid including outside interconnectors is 95.92 GW. The load value at each cluster at that moment is shown in Table 1. Clusters that start from 50000 represent buses located in other European countries where all other clusters are located inside Germany.

Table 1: Loads values at maximum demand including interconnectors

| Cluster | Load [MW] | Cluster | Load [MW] |
|---------------|-----------|---------------|-----------|
| cluster_23956 | 0 | cluster_40009 | 3868.11 |
| cluster_27046 | 11.40 | cluster_50000 | 1110 |
| cluster_40000 | 5244.21 | cluster_50001 | 170 |
| cluster_40001 | 4586.40 | cluster_50002 | 5481 |
| cluster_40002 | 6169.56 | cluster_50003 | 13496 |
| cluster_40003 | 13681.02 | cluster_50004 | 666 |
| cluster_40004 | 4529.62 | cluster_50005 | 0 |
| cluster_40005 | 8787.29 | cluster_50006 | 6197 |
| cluster_40006 | 3372.40 | cluster_50007 | 4574 |
| cluster_40007 | 8788.69 | cluster_50008 | 507 |
| cluster_40008 | 4678.34 | Total | 95918.04 |

3.2.2 Maximum Demand Including Loads Only Inside Germany

Like before, after performing data analysis using Python, the maximum load including loads only inside Germany occurs in 2020 at hour number 66 which will be Thursday, 2 January 2020 at 19:00. The value of this maximum demand for the whole grid is 77.94 GW. The loads values can be seen in Table 2.

Table 2: Loads values at maximum demand only inside Germany

| Cluster | Load [MW] | Cluster | Load [MW] |
|---------------|-----------|---------------|-----------|
| cluster_23956 | 5.45 | cluster_40009 | 4746.96 |
| cluster_27046 | 13.63 | cluster_50000 | 0 |
| cluster_40000 | 6480.06 | cluster_50001 | 0 |
| cluster_40001 | 5631.70 | cluster_50002 | 0 |
| cluster_40002 | 7705.01 | cluster_50003 | 0 |
| cluster_40003 | 16475.87 | cluster_50004 | 0 |
| cluster_40004 | 5281.95 | cluster_50005 | 0 |
| cluster_40005 | 10944.35 | cluster_50006 | 0 |
| cluster_40006 | 4134.66 | cluster_50007 | 0 |
| cluster_40007 | 10864.90 | cluster_50008 | 0 |
| cluster_40008 | 5659.41 | Total | 77943.95 |

3.3 Aggregation of Generators

In This section, generators will be aggregated and at each cluster, there will be three generators types: wind, solar, and conventional. To do this, in the case of wind and solar, the ratings and control mode of the generators shall be determined. However, for conventional machines, in addition to the rating of the machine, the inertia constant H plays a vital role in the model. Hence, to add up wind or solar generators at the same cluster, their rated power is just added up. But in the case of synchronous machines, the rated power will be added up and the inertia shall be added up but adjusted to the scale of each machine.

In other words, at each cluster, many solar, wind, and synchronous machines will be connected and they have to be added up to result in one generator per type. As there are many conventional generation technologies, typical values for the inertia constant H were taken from the literature. For example, combined cycle gas turbines, simple cycle gas turbines (steam turbines), hydro-power plants, and

non-converter-based technologies were set to inertia constant values 5.5,7,3, and 0, respectively [26]. Table 3 shows the generators connected to cluster 40000.

Table 3: Generators per source at cluster 40000 to be aggregated

| Source | Rated Power [MW] | H [s] |
|------------|------------------|-------|
| Gas | 1371.44 | 5.50 |
| Lignite | 61.71 | 7.00 |
| Nuclear | 1360 | 7.00 |
| Biomass | 824.05 | 7.00 |
| Coal | 1405.50 | 7.00 |
| Hydro | 271.23 | 3.00 |
| Solar | 3752.35 | 0 |
| Wind | 6734.11 | 0 |
| Geothermal | 17.11 | 5.50 |

The overall inertia constant of generators of different rated powers is calculated as follows:

$$H_{tot} = \frac{H_1 P_1 + H_2 P_2 + \dots + H_n P_n}{P_1 + P_2 + \dots + P_n} \quad (15)$$

Where H_{tot} is the overall inertia constant for all combined synchronous machines at a specific cluster. H_n is the inertia constant at machine n. P_n is the rated power in MW of machine n.

After aggregating all generators according to the rules mentioned before, the overall solar, wind, and conventional generator ratings will be as in Tables 4, 5, and 6. These full capacities will be later used to determine the actual generation dispatch of each unit at each cluster, where the total generation will be set proportionally with the capacity of each one.

Table 4: Aggregated solar generators at each cluster

| Cluster | Full Capacity [MW] |
|---------|--------------------|
| 23956 | 3.04 |
| 27046 | 25.71 |
| 40000 | 3752.35 |
| 40001 | 5415.59 |
| 40002 | 8897.32 |
| 40003 | 4642.65 |
| 40004 | 2758.07 |
| 40005 | 6169.05 |
| 40006 | 4489.83 |
| 40007 | 4643.80 |
| 40008 | 3668.72 |
| 40009 | 5110.81 |

It is important to mention that clusters outside Germany that starts from 50000 till 50008 are not taken into account. Instead, they will be replaced by one static generator at each cluster that generates that exact power value at the moment of maximum demand. Also, all power plants are set in a way that operates at 0.95 PF lagging, so this also takes into account the reactive power. For wind and solar generators, the inertia constant H is neglected in this research as PowerFactory does not have the option of H in the wind and solar generator models. Furthermore, the inertia of inverter-based resources is very small.

Table 5: Aggregated wind generators at each cluster

| Cluster | Full Capacity [MW] |
|---------|--------------------|
| 23956 | 3.60 |
| 27046 | 1.80 |
| 40000 | 6734.11 |
| 40001 | 3372.04 |
| 40002 | 713.72 |
| 40003 | 5314.56 |
| 40004 | 11296.63 |
| 40005 | 1293.69 |
| 40006 | 9266.35 |
| 40007 | 5207.93 |
| 40008 | 13110.62 |
| 40009 | 5761.51 |

The accumulated synchronous machines per cluster is also shown in Table 6. it is important to mention that also the inertia constant H is considered in the table, and as before the rated PF is 0.95 lagging. Therefore, the rating of the reactive power will be also included.

Table 6: Aggregated conventional generators at each cluster

| Cluster | Full Capacity Power [MW] | H_{tot} [MJ/MW] |
|---------|--------------------------|-------------------|
| 23956 | 350.10 | 7.00 |
| 27046 | 6.17 | 6.95 |
| 40000 | 5904.33 | 6.087 |
| 40001 | 3233.35 | 5.64 |
| 40002 | 11929.46 | 5.39 |
| 40003 | 28495.82 | 6.38 |
| 40004 | 6709.39 | 6.43 |
| 40005 | 9281.20 | 5.955 |
| 40006 | 4465.61 | 6.00 |
| 40007 | 10063.71 | 6.16 |
| 40008 | 10410.47 | 6.27 |
| 40009 | 12578.82 | 6.74 |

The inertia constant H is calculated here based on active power P , not apparent power S , and using PowerFactory this can be chosen as an option and it will be adjusted automatically based on the apparent power using the rated value of the power factor. Each cluster has its complete rated parameters whether it's the load, transmission lines, transformer impedance, or generators. As mentioned before, now, each cluster looks like Figure 19.

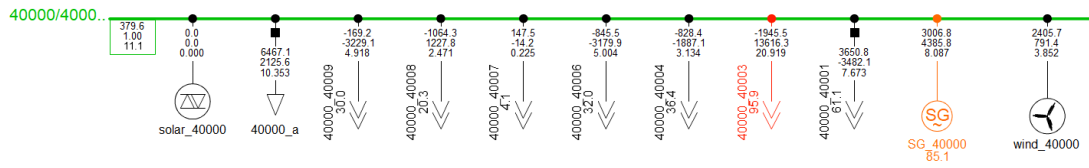


Figure 19: Load flow at cluster 40000 at the max. demand inside Germany case

After the aggregation is complete. The general shape of each cluster contains one synchronous machine, one wind generator, a solar generator (implemented as a static generator), load, transmission lines, and other components in some cases.

3.4 Generation Dispatch

Now the dispatch of generation has to be investigated at the maximum demand points to complete the steady state model and be able to run the load flow to move to the next step which is transient stability analysis. The full capacity of each unit was determined in the previous section. However, it does not mean that the system will operate at these maximum values, the actual generation dispatch will be determined in this section.

3.4.1 Generation Dispatch at Maximum Demand Considering Loads Outside Germany

The maximum demand considering loads outside Germany occurs on 19-Feb-2020, Wednesday at 13:00 and its value is 95.92 GW.

Using Figure 20, At that moment, the total generation is around 96.11 GW. Solar generation contributes with 11.84% of the total generation. Where the wind makes around 37.8% of the total generation and the rest comes from synchronous machines. Therefore, the generation by solar, wind, and conventional is approximately 10.94 GW, 36.32 GW, and 48.85 GW, respectively. This total generation at that moment will be distributed proportionally according to the capacity of the generator. Thus, the dispatch at the moment of maximum demand considering loads outside Germany at each cluster will be as illustrated in Table 7.

Table 7 includes the generation pattern for the whole system, so it contains the summary of actual power values that will be injected into the grid at the required time. Also, taking into consideration the power factor which is 0.95 lagging, the dispatch of the reactive power injected into the grid will be calculated accordingly.

Table 7: Dispatch at the maximum demand considering outside Germany

| Cluster | Solar [MW] | Wind [MW] | Synchronous Gen. [MW] |
|---------|------------|-----------|-----------------------|
| 23956 | 0 | 0 | 0 |
| 27046 | 5.67 | 1.07 | 2.92 |
| 40000 | 828.18 | 3987.30 | 2788.53 |
| 40001 | 1195.27 | 1996.60 | 1527.06 |
| 40002 | 1963.72 | 422.60 | 5634.10 |
| 40003 | 1024.68 | 3146.78 | 13458.15 |
| 40004 | 608.73 | 6688.79 | 3168.74 |
| 40005 | 1361.57 | 766.00 | 4383.37 |
| 40006 | 990.95 | 5486.65 | 2109.04 |
| 40007 | 1024.93 | 3083.64 | 4752.94 |
| 40008 | 809.72 | 7331.98 | 4916.71 |
| 40009 | 1128.67 | 3411.42 | 6106.13 |
| Total | 10942.1 | 36321.73 | 48847.69 |

The interconnectors are not included in the table because they are not flowing any power now in the German power pool. On the contrary, as shown before, they draw power from the German grid and that is why the load is significantly larger than in section 3.5.2.

3.4.2 Generation Dispatch at Maximum Demand Only Considering Loads Only Inside Germany

As discussed before, the maximum load considering only loads inside Germany occurs on 02-Jan-2020, Thursday at 19:00 and its value is 77.94 GW.

Using Figure 21, At that moment, the total generation is around 78.05 GW. Solar generation contributes with 0% simply because there is no sun. The wind

makes around 28.91% of the total generation and the rest comes from conventional. Therefore, the generation by solar, wind, and conventional is approximately 0, 23.42 GW, and 54.62 GW, respectively.

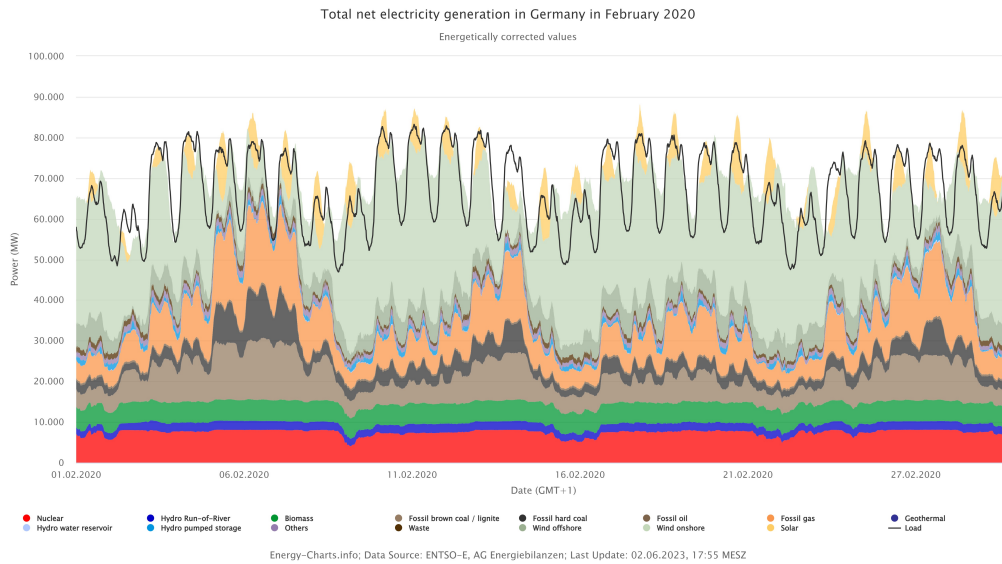


Figure 20: Generation dispatch in February 2020 [4]

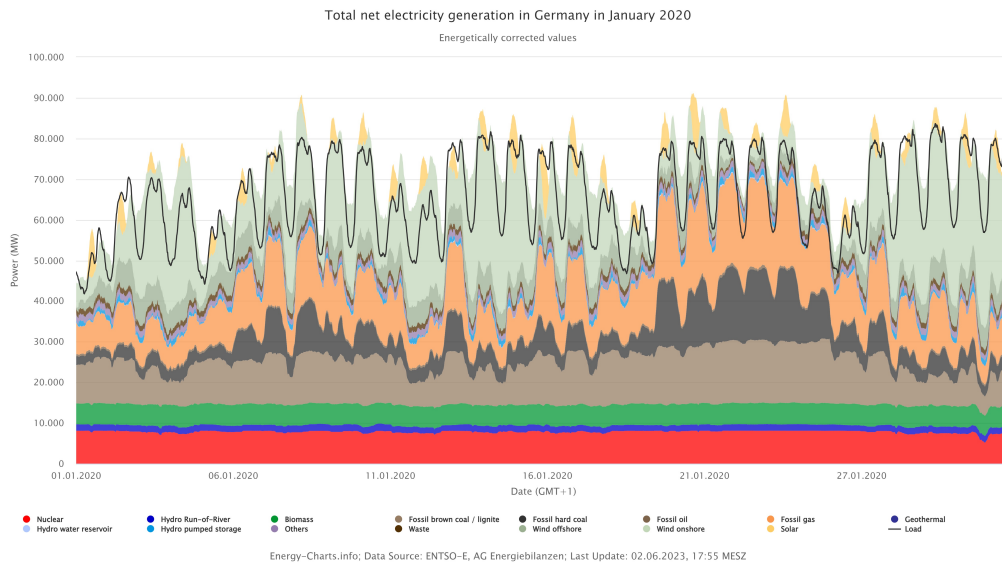


Figure 21: Generation dispatch in January 2020 [5]

This total generation at that moment will be distributed proportionally according to the capacity of the generator. Thus, the dispatch at the moment of maximum load inside Germany at each cluster is in Table 8.

At that moment, it is important to mention that there is power flowing inside the German grid from interconnector 50005 which comes from outside the country and the value of this power is 681 MW. All of that will result in a generation of 78.04 GW in the German power pool at that moment.

Table 8: Generation dispatch at maximum demand inside Germany

| Cluster | Solar [MW] | Wind [MW] | Synchronous Gen. [MW] |
|---------|------------|-----------|-----------------------|
| 23956 | 0 | 0 | 0 |
| 27046 | 0 | 0.64 | 2.55 |
| 40000 | 0 | 2410.20 | 2090.96 |
| 40001 | 0 | 1206.88 | 914.20 |
| 40002 | 0 | 255.45 | 6330.16 |
| 40003 | 0 | 1903.42 | 20359.90 |
| 40004 | 0 | 4043.17 | 1082.76 |
| 40005 | 0 | 463.02 | 5875.88 |
| 40006 | 0 | 3316.52 | 293.00 |
| 40007 | 0 | 1863.97 | 6046.60 |
| 40008 | 0 | 4692.42 | 3100.24 |
| 40009 | 0 | 2062.10 | 9050.28 |
| Total | 0 | 23423.80 | 54621.06 |

Now, after the grid is modelled, the values of loads are determined at the maximum points of operation, and the actual generation dispatch is distributed. The steady-state grid is ready for load flow running. In the next section, study cases and scenarios will be discussed.

3.5 Study Cases & Scenarios

Based on section 2.4, transient stability scenarios will be defined, simulated, and the results will be verified and discussed. In the first case, the scenarios will be simulated using currently-used controllers for WEC and solar generators. In the second case, these controllers will be replaced by VSM.

The following scenarios will be investigated:

1. Short circuit fault at the synchronous machine at cluster 40003 and a fault clearance to happen due to instantaneous protection (after 100 ms): This represents **Case 1** in section 2.4, it will be implemented using a damper winding and without a damper winding.

Relevance: The synchronous machine at cluster 40003 generates the largest amount of power among all generators (20.36 GW at maximum demand inside Germany case and 14.36 GW when including the loads outside Germany case) which implements a partial shutdown (brownout). This will decrease the input power P_m drastically creating the biggest possible mismatch between the input power P_m and the output P_e that can happen due to a generator's outage or an aggregated generation unit according to equation (3). Therefore, it will create the largest oscillation in the rotor angle representing the frequency of the system will be in its most critical generator outage case. The location of cluster 40003 is marked in the grid in Figure 22.

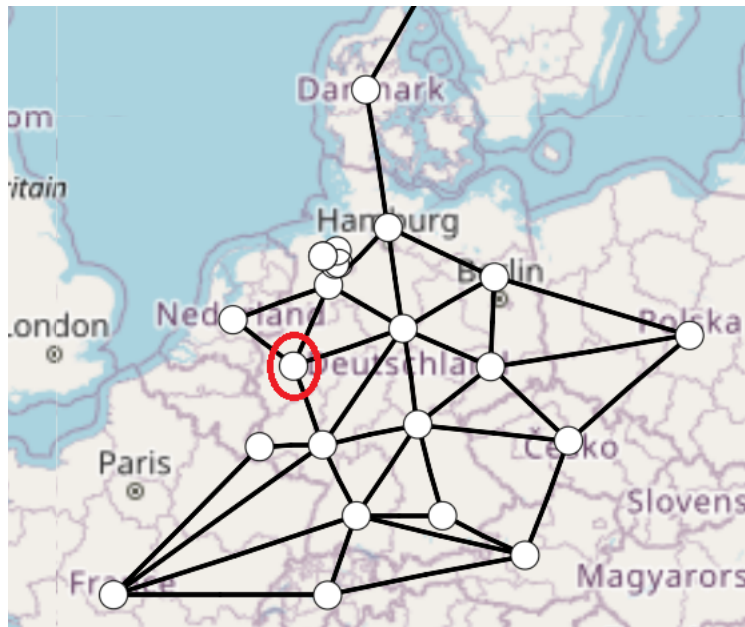


Figure 22: Location of cluster 40003

In reality, this can happen due to a **cascaded failure in generation units at cluster 40003 due to losing synchronism in that region.**

2. Load shedding at different scenarios: different load shedding scenarios will be investigated including shedding of the maximum load at cluster 40003 which makes 13.46% of the total load in the max demand case including loads outside Germany and 20.6% in the case of max demand considering loads only inside Germany. This represents **Case 2** in section 2.4.

Relevance: Disconnecting the biggest load results in the biggest mismatch between the input power P_m and the output power P_e according to equation (3) in the load shedding case because the output power will drastically decrease. The location of the biggest load at cluster 40003 is also shown in Figure 22. Thus, it represents the most critical case of load shedding. Hence, the oscillation of the rotor angle that represents the frequency of the system will be in its most critical load disconnection case. In reality, this can happen when **disconnecting a large served area in the German grid.** Aside from that, other different scenarios of load-shedding will be studied like 7% or 8% load-shedding scenarios to find the load-shedding point where the system with VSM will be able to survive and still operate within the steady-state values, and where the system without VSM would fail.

3. Short circuit fault in the middle of the line 40000-40001 and disconnecting it due to instantaneous protection (after 100 ms): This represents **Case 3** in section 2.4.

Relevance: This line is the highest loaded line in the power grid so a significant amount of power flows through it. It connects cluster 40000 with cluster 40001. When a short circuit fault occurs, the load fed by this line will be replaced by a short circuit (ideally the load is equal to 0 now) which will create a huge mismatch in the input power and the output power at the fault moment as explained before. The location of line 40000-40001 is marked in the grid shown in Figure 23.

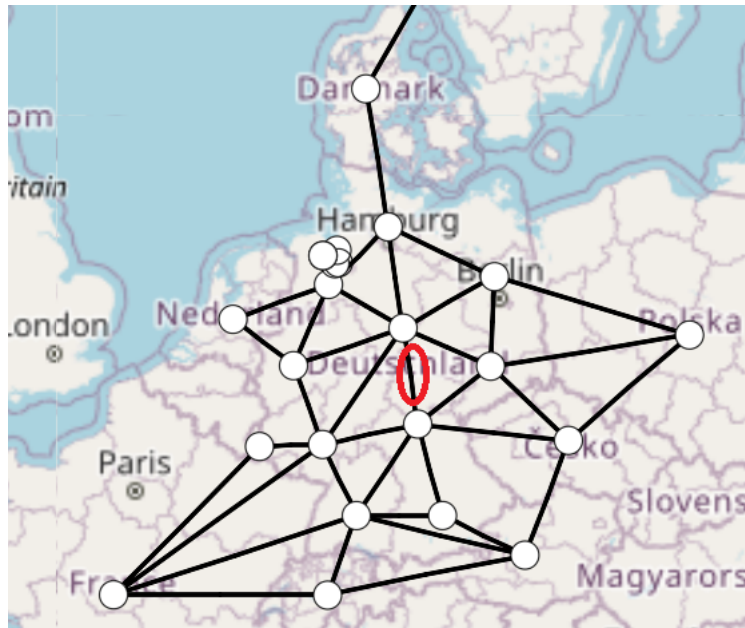


Figure 23: Location of line 40000-40001

Case 4 in section 2.4 will not be investigated because in the available grid model, transmission lines that connect clusters are aggregated in one equivalent transmission line, which means parallel transmission lines do not exist to switch one of them out.

In the next chapter, the results will be shown and discussed at the two maximum demand points considering loads only inside Germany, and when the total demand including loads outside Germany is considered. Finally, the results' compliance with the European grid code will be verified and discussed.

4 Results & Discussion

This section will present the results of the previously defined scenarios in section 3.5.

4.1 At Maximum Demand when Loads inside Germany only are Considered

In each scenario, the results will be shown for a system without VSMs, and another which is totally replaced with VSMs, the synchronverter results will be shown for a case where it verifies its similarity to VSM. The frequency response and the voltage response at each scenario will be represented for the buses that correspond to the disturbance. That means if a load-shedding is applied at a load connected to bus X, the frequency and voltage response will be represented at bus X. The reference machine is set to be the synchronous machine connected to 40003 which has the highest capacity. This is applicable for both systems with and without VSM.

4.1.1 Short Circuit at Synchronous Machine 40003 and Fault Clearance after 100 ms

Disconnection of a large aggregated synchronous generator (20.36 GW) is applied in this case which represents a partial shutdown in the grid. In this case, the synchronous machine experiences a three-phase fault at its terminal at a time of 10 seconds. It can be seen in Figure 24 that before second 10, both systems were operating within the steady-state limit. However, after the short circuit happens, an instantaneous main protection will operate to clear the fault and isolate the synchronous machine. It can be seen that the system without VSM collapses drastically, where its frequency decays fast. On the other hand, the system with VSM can survive the disturbance but it will operate outside the steady-state limits (52.69 Hz). The primary control kicks in within this period and adjusts the frequency. Nevertheless, tuning the damper winding parameter can solve this problem. It is important to mention in the case of maximum demand considering only loads inside Germany, the solar generation is zero because it occurs at a time when there is no solar radiation, so the benefit from VSM in solar converters is not available. From Figure 24, it can be seen that the system with VSM outperforms the system without VSM.

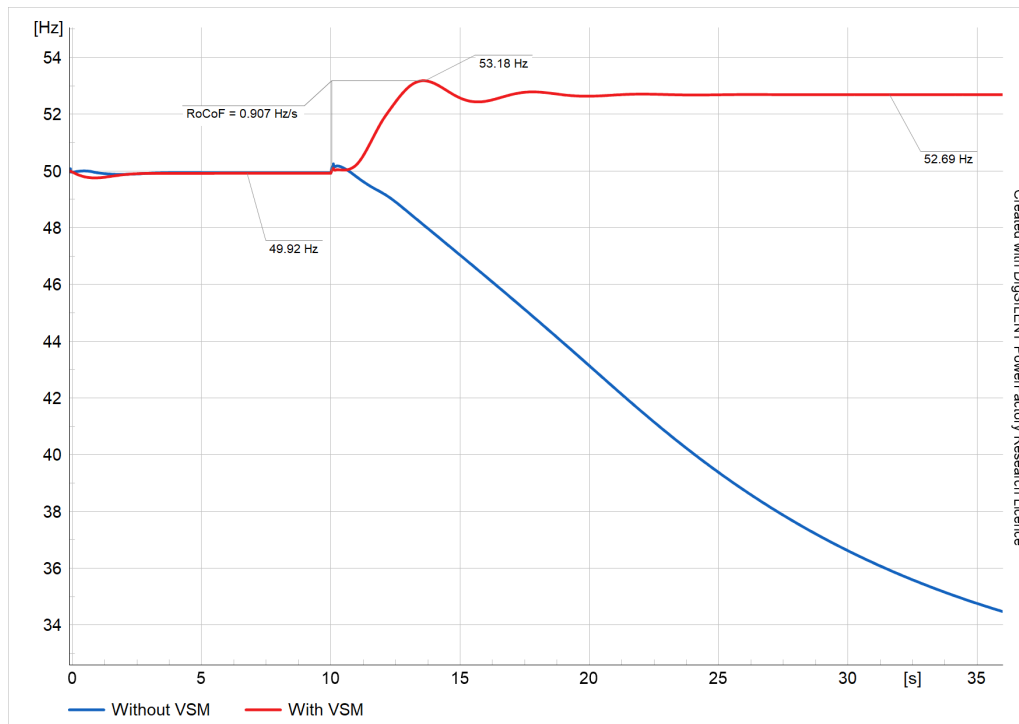


Figure 24: Frequency response for case 4.1.1

The voltage response is shown in Figure 25, the voltage of the bus at the moment of the fault drops to zero considering a zero fault impedance. The recovery of the voltage to its normal operational level of the system with VSM is faster than in the system without VSM which is called the fault ride through time (FRT). After the fault is cleared, the system with VSM gets back to its steady-state operational value, but the one without VSM keeps declining.

Adding a damper winding at the reference machine and increasing its value empirically leads to stabilizing the system with VSM. However, the value that stabilizes the system is big and not quite realistic, but it gives a theoretical indication that the system could be brought to stability by tuning some parameters. After adding a damper winding of 2.5 p.u. to the reference machine, it can be seen in Figure 26 that after the fault, the frequency of the system with VSM is brought back to the steady-state limit (50.09 Hz), but it was not able to restore the system without VSM. The damper winding stops the system without VSM from decaying more for both values of frequency and voltage. However, it keeps oscillating outside the steady-state limit of frequency.

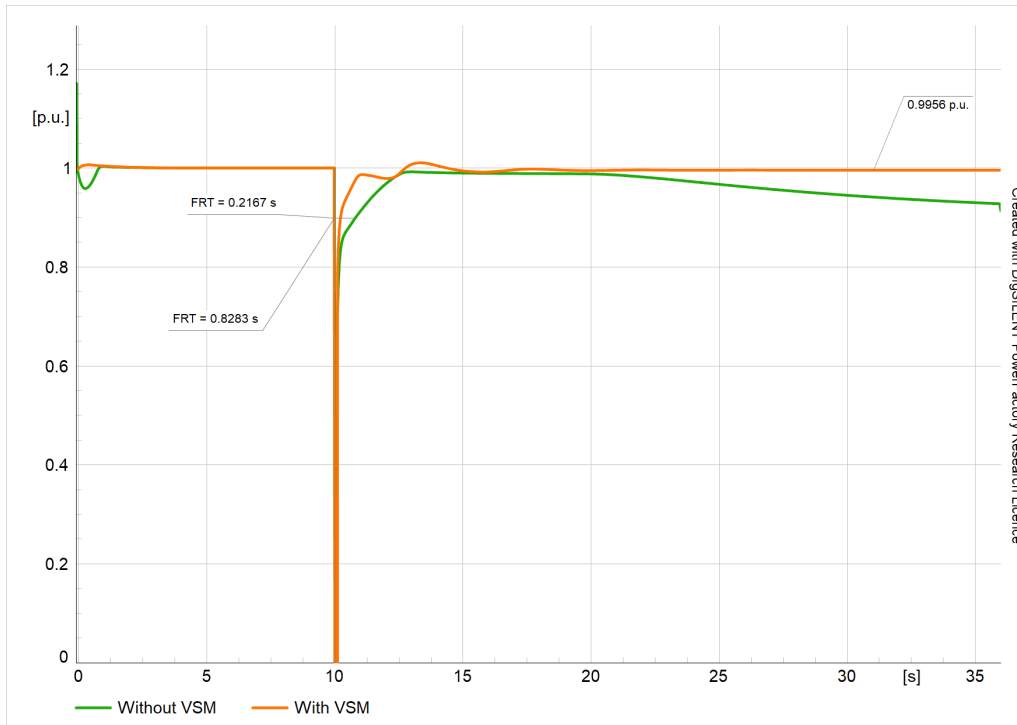


Figure 25: Voltage response for case 4.1.1

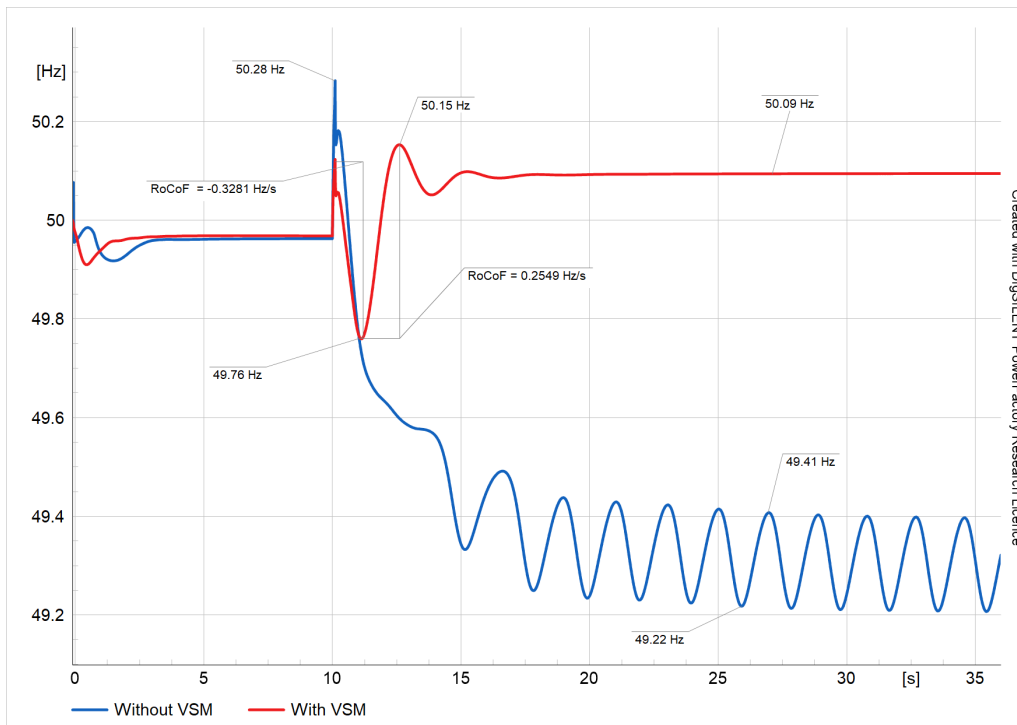


Figure 26: Frequency response for case 4.1.1 with damper winding tuning

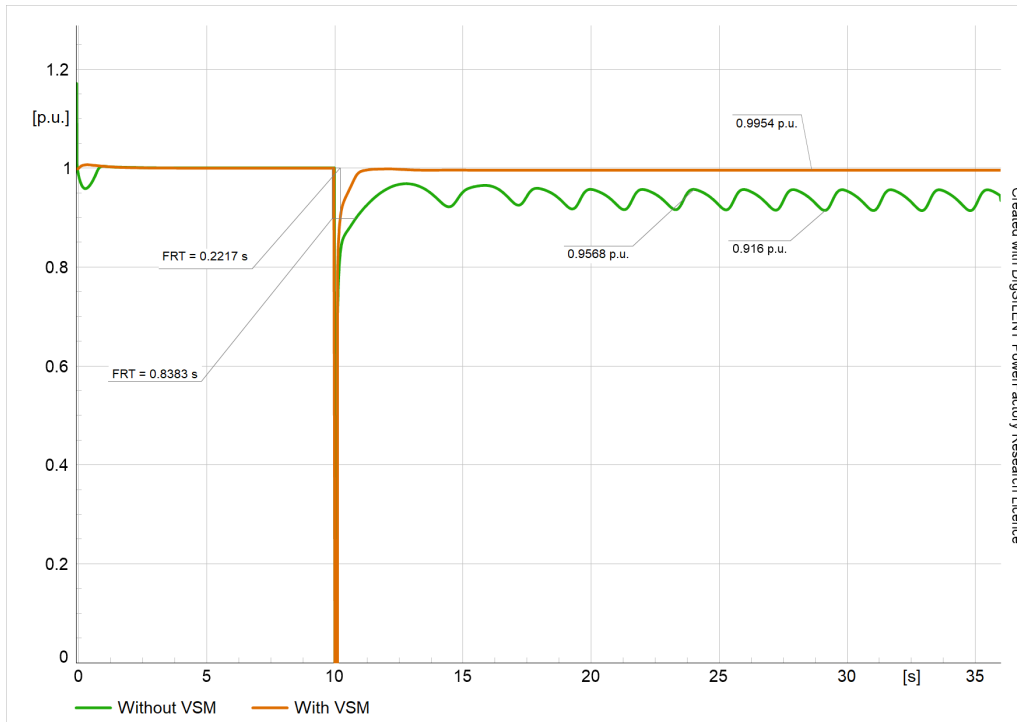


Figure 27: Voltage response for case 4.1.1 with damper winding tuning

The results of disconnecting the synchronous machine at cluster 40003 after a severe short-circuit are summarized in Table 9.

Table 9: Results for disconnecting synchronous machine 40003 after a short-circuit

| Quantity | VSM | No VSM | VSM (with damper) | No VSM (with damper) |
|----------------|-------|-----------|-------------------|-------------------------|
| OS [Hz] | 53.18 | NA | 50.15 | 50.28 |
| US [Hz] | NA | NA | 49.76 | NA |
| RoCoF 1 [Hz/s] | 0.91 | NA | -0.33 | NA |
| RoCoF 2 [Hz/s] | NA | NA | 0.25 | NA |
| f_{ss} [Hz] | 52.69 | collapsed | 50.09 | oscillating see Fig. 26 |
| FRT [s] | 0.22 | 0.83 | 0.22 | 0.84 |

From the results above, it can be shown that before adding the damper winding, the instantaneous frequency values do not comply with the ENTSO-E grid code in

section 2.2, where the OS value which is 53.18 Hz exceeds the 800 mHz deviation. This can result in a trip in the over-frequency protection [14]. However, After adding the damper winding, all instantaneous values of the OS and US in both systems with VSM and without VSM comply with the ENTSO-E grid code. Hence, no action of interruption will be taken. For RoCoF values, none of them exceed an absolute value of 1.25 Hz/s. Therefore, all power generating-modules shall remain stable and connected to the grid. For f_{ss} values and before adding the damper winding the power generating modules will not be able to stay connected to the grid for an unlimited time where the f_{ss} is 52.69 which is outside the range 49 Hz - 51 Hz which allows the generator to stay connected to the grid for an unlimited time. However, After adding the damper winding, f_{ss} is equal to 50.09 which not only allows generators to stay connected to the grid for unlimited time but also lies within the steady-state frequency deviation.

4.1.2 Load Shedding

The load shedding values were chosen based on the actual load values of each cluster. The load values start increasing gradually until reaching a final value that violates the allowable steady-state value of either frequency or voltage. First, 7% load-shedding at 40008 cluster is performed and the frequency response results are shown in Figure 28. It can be noticed that both responses with and without VSM are still operating within the steady-state frequency limits after the disturbance is applied. However, the performance of the system with VSM is better than without VSM regarding RoCoF and OS values.

Figure 29 shows the voltage response of the 7% load-shedding case at a time of 10s. It can be noticed that the performance of both systems with and without VSM is very similar and there is no significant difference. That proves what is mentioned before, that the VSM's main role is to compensate for the absence of the inertia and it does not play a vital role in voltage response. After the disturbance is applied at a time of 10s, there is a slight increase in the voltage value. That is because after disconnecting a load, the load current becomes smaller and therefore the voltage drop across the lines becomes smaller which results in a slightly higher value at the receiving end.

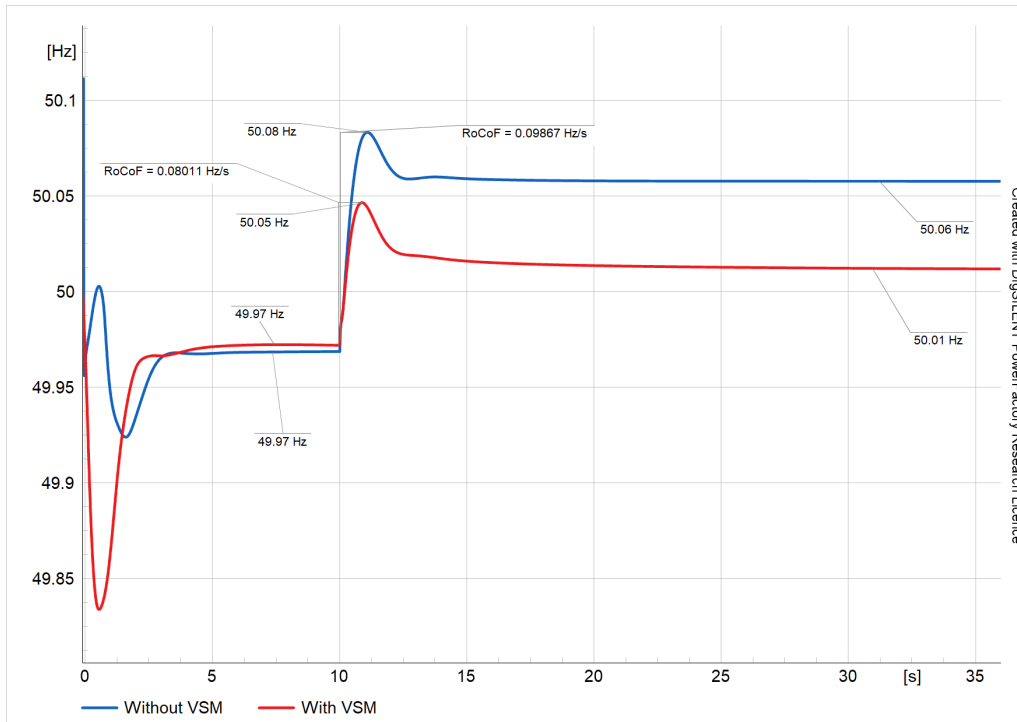


Figure 28: Frequency response at 7% load shedding of total load

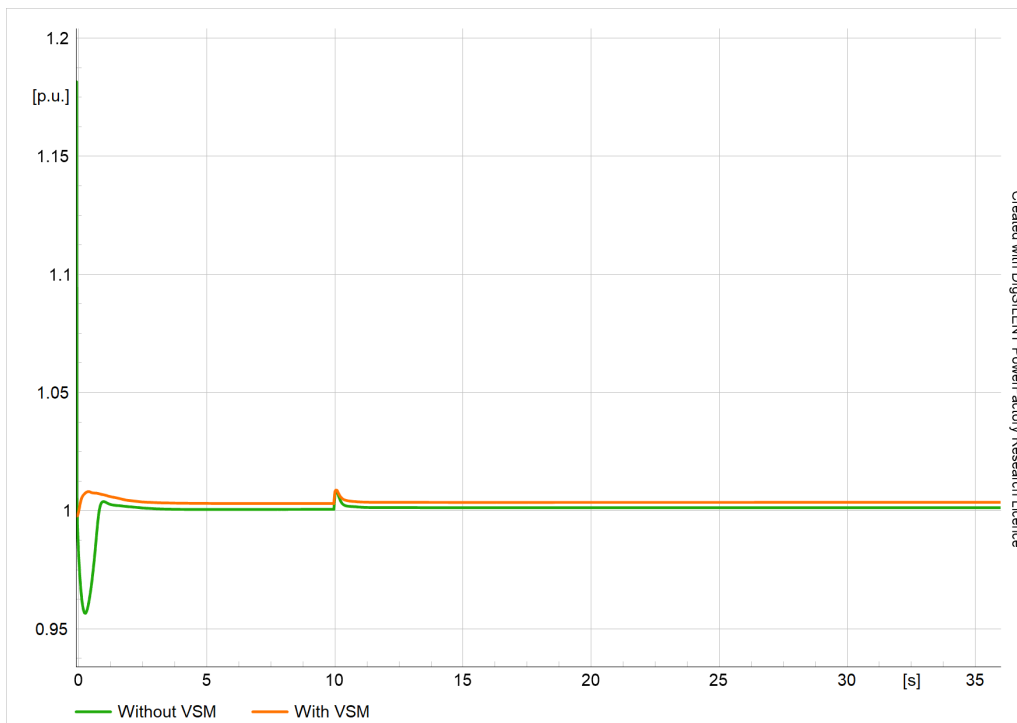


Figure 29: Voltage response at 7% load shedding of total load

Figure 30 shows the frequency response of a 8% load-shedding at cluster 40000. It can be seen from the graph that both systems were able to survive the load-shedding disturbance, which means they still have a frequency within the steady-state operational limit. However, the RoCoF and OS values with VSM are better than those without VSM.

Figure 31 shows the voltage response of the 8% load-shedding scenario. After disconnecting the load, and since its value is bigger than the 7% scenario, the voltage rise will be significantly noticeable. Since the load current decreases after disconnecting the 8% load and the reactive power drawn by this inductive load becomes less. A voltage rise is observed at the receiving end of the bus bar.

Finally, Figure 32 represents a turning point in the course of events. The frequency response of the maximum possible load shedding scenario, which is the load connected to cluster 40003 and makes 20.6% of the total demand where its value is 16.48 GW. After the load shedding at a time of 10s, the VSM was able to succeed in maintaining its steady-state stability limit when disconnecting the maximum running demand, while the system without VSM is going further from the steady-state limit than the previous scenario (8% load shedding) and reaches a frequency value of 50.22 Hz. In Figure 33, the voltage response of the 20.6% load shedding case is shown. Just as mentioned in the previous load-shedding scenarios the performance of both systems (with and without VSM) is acceptable.

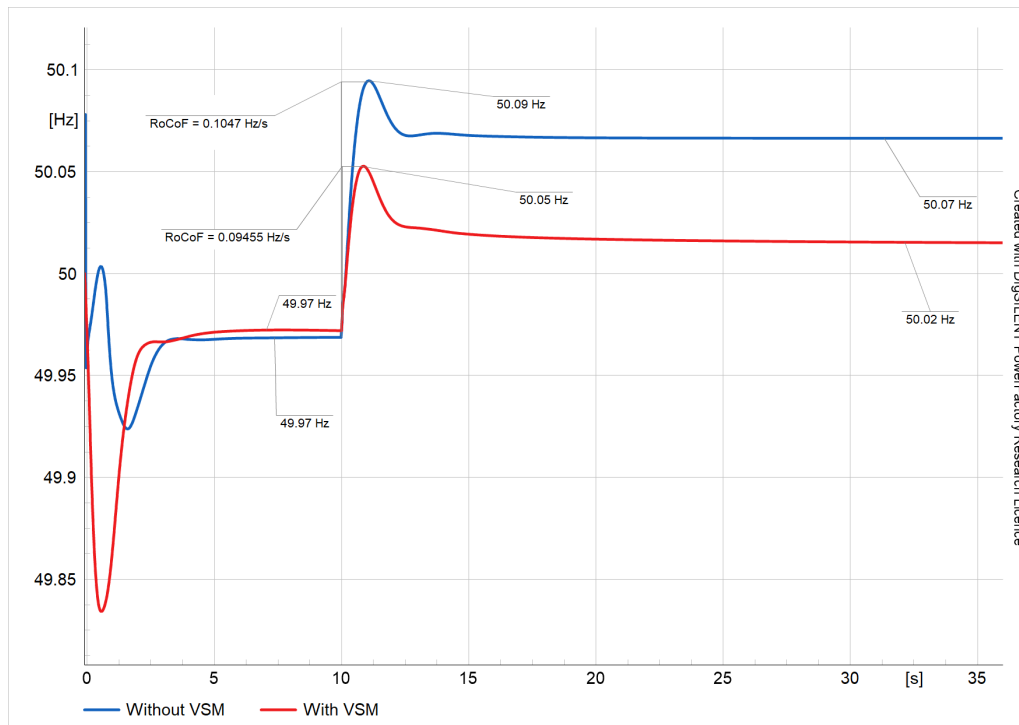


Figure 30: Frequency response at 8% load shedding of total load

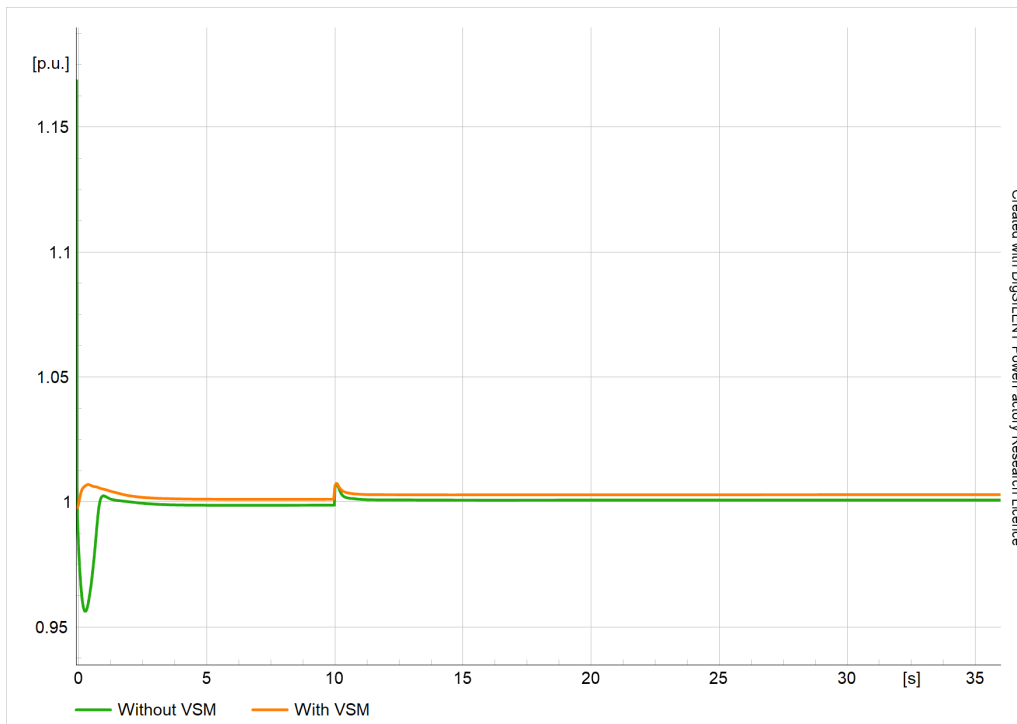


Figure 31: Voltage response at 8% load shedding of total load

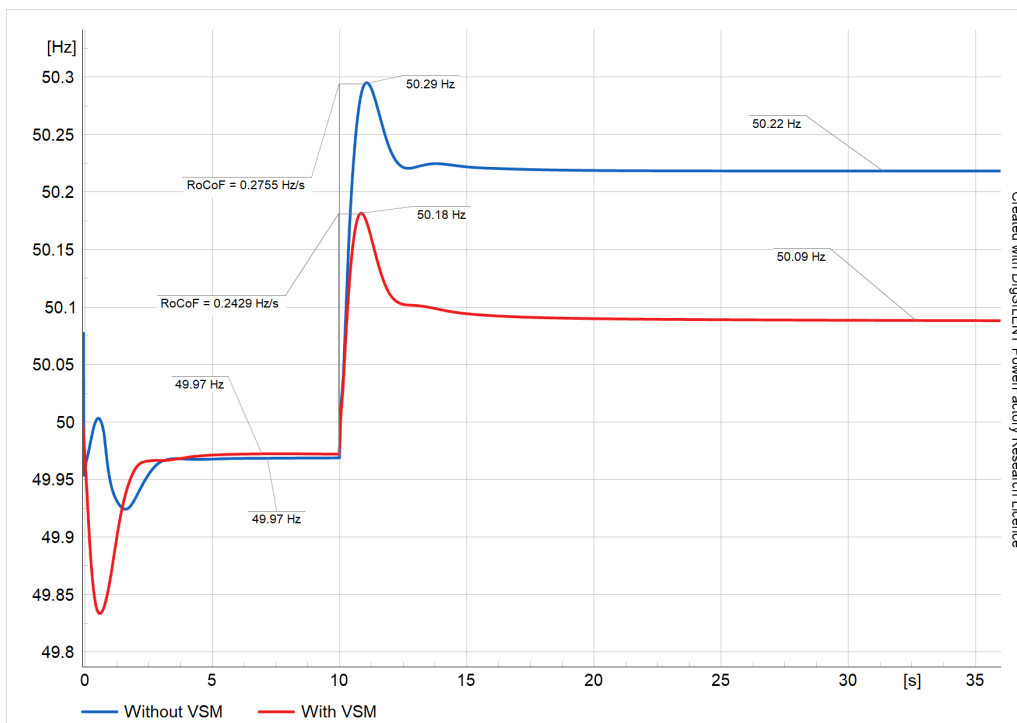


Figure 32: Frequency response at 20.6% load shedding of total load

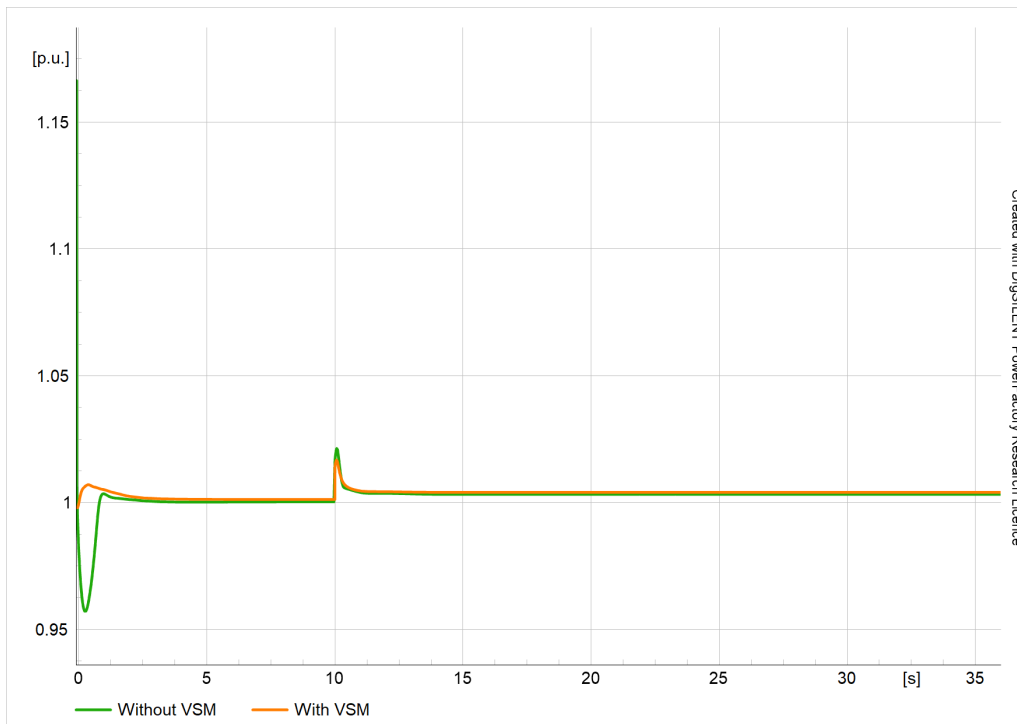


Figure 33: Voltage response at 20.6% load shedding of total load

4.1.3 Using Synchronverters

Taking into consideration a system fully replaced with a synchronverter, it can be also seen in Figure 34 that in the case of 20.6% load shedding, the system with synchronverters was able to run after the disturbance at a frequency of 50.05 Hz, which reflects a good performance of the system and lies within the steady-state frequency region. This is because of the similarity in the behaviour of the VSM and synchronverter since it uses torque instead of power as measured and reference values as mentioned in the synchronverter subsection in the theory chapter.

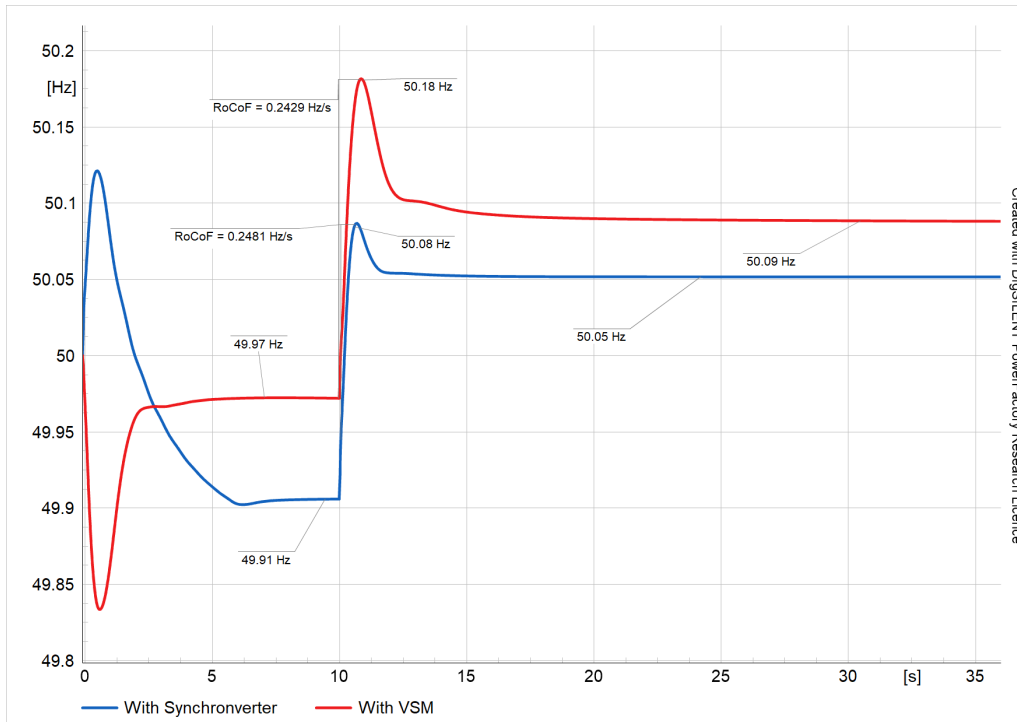


Figure 34: Frequency response of VSM and synchronverter for 20.6% load-shedding

The summary of 20.6% load-shedding results is shown in Table 10.

Table 10: Results for 20.6% load-shedding of total load

| Quantity | VSM | No VSM | Synchronverter |
|---------------|-------|--------|----------------|
| OS [Hz] | 50.18 | 50.29 | 50.08 |
| RoCoF [Hz/s] | 0.24 | 0.28 | 0.25 |
| f_{ss} [Hz] | 50.22 | 50.09 | 50.05 |

From the results above, it can be seen that all values whether they are instantaneous OS, RoCoF, or f_{ss} lie within the ENTSO-E grid code limits. Hence, the generators will not trip for the OS values since they lie within the range of 49 Hz - 51 Hz, and they will be able to stay connected for an unlimited time. Nevertheless, f_{ss} exceeds the range of maximum steady-state frequency deviation which is 49.2 Hz - 50.8 Hz [14]. Based on that, the performance of the system with GFCs (VSMs and synchronverters) is significantly better than the one with GFCs. However, the difference in the performance of the system with VSMs and with synchronverters Table 10.

The results of load-shedding also comply with the literature as the steady-state frequency using GFCs has a steady-state frequency that lies within the maximum deviation of steady-state frequency and outperforms in this aspect the system without VSM [7].

4.1.4 Disconnecting Line 40000-40001, 100 ms after a Short Circuit Fault in the Middle of the Line

In Figure 35, the frequency response of disconnecting the line 40000-40001 which connects cluster 40000 and 40001 is shown. It can be seen that both systems with and without VSM return to their steady-state values limit after the short circuit occurs at a time of 10s. However, the RoCoF and OS values show the superior ability of VSM to dampen the OS significantly and to reduce the RoCoF in a very effective way. It is important to mention that in this case, the system does not lose or gain any amount of input or output power since no loads or generators get disconnected. What happens actually, is that a highly-loaded line gets disconnected and its power flow is re-distributed to other lines. That's why there is almost no increase or decrease in the steady-state frequency value before and after the large disturbance.

The voltage response is shown in Figure 36. Unlike the case of severe short circuit fault at a generator's terminals, the voltage here does not drop to zero, that is because when the short circuit occurs at the middle of the line, the bus bar connected to the faulted line is not directly connected to the ground, but it has a small voltage that is equal to the value of the fault current multiplied by half of the impedance of the line which results in the non-zero voltage value. The FRT time in a system with VSM is shorter than in the system without VSM. Thus, the performance in the FRT of the VSM system outperforms the one without VSM.

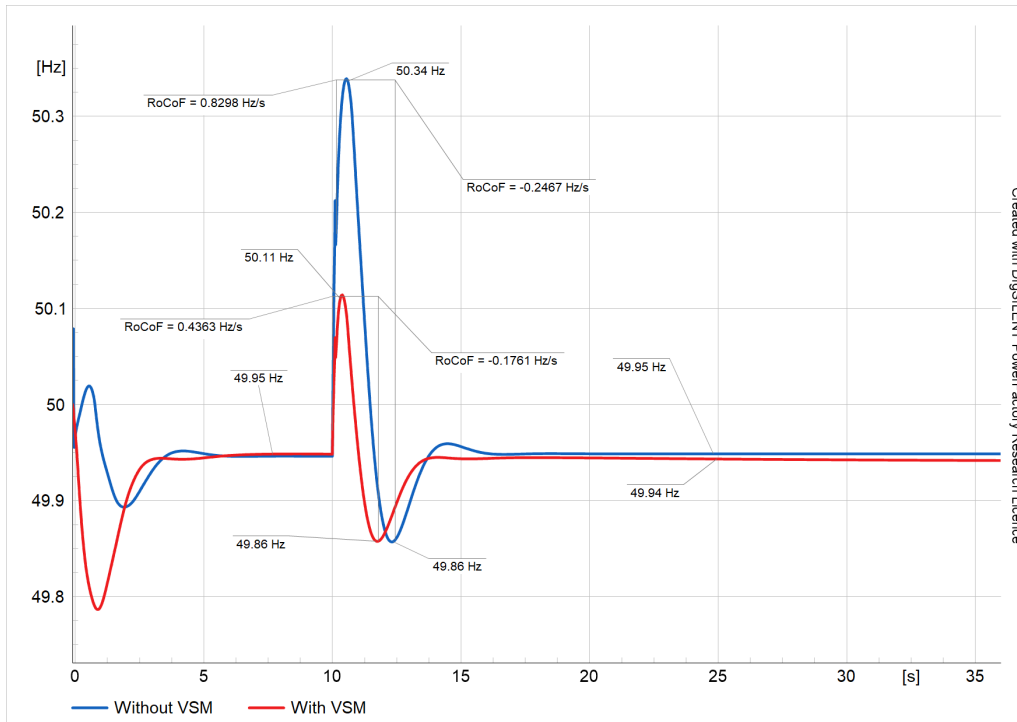


Figure 35: Frequency response for the case in 4.1.4

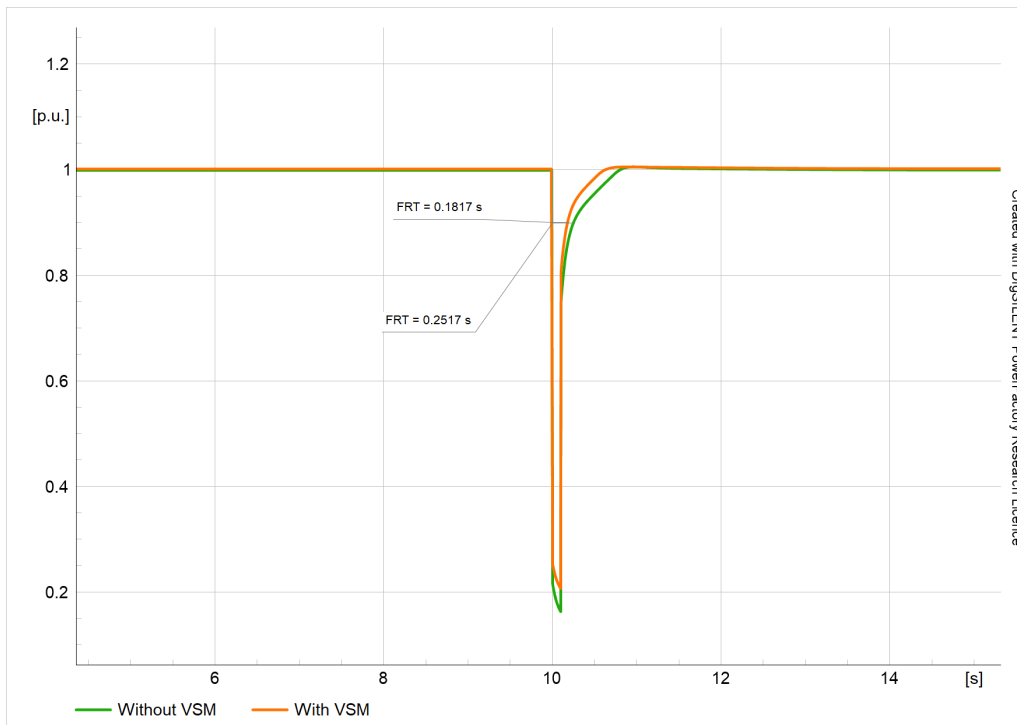


Figure 36: Voltage response for the case in 4.1.4

The results of this scenario are shown in Table 11.

Table 11: Results for shorting and disconnecting line 40000-40001

| Quantity | VSM | No VSM |
|----------------|-------|--------|
| OS [Hz] | 50.11 | 50.34 |
| US [Hz] | 49.86 | 49.86 |
| RoCoF 1 [Hz/s] | 0.44 | 0.83 |
| RoCoF 2 [Hz/s] | -0.18 | -0.25 |
| f_{ss} [Hz] | 49.94 | 49.95 |
| FRT [s] | 0.18 | 0.25 |

It can be seen that all results comply with the ENTSO-E grid code. The instantaneous values (OS and US), RoCoF, and f_{ss} are located within the limits [14].

However, referring to the literature. It is expected of the system with VSM to have better performance than the system without VSM in the scenario of faulting a line a disconnecting it [7], and that is shown in the results above.

4.2 At Maximum Demand Considering Loads outside Germany

One more time, the results will be shown for a system without VSMs, and another which is replaced with VSMs. The frequency response and the voltage response in each scenario will be represented for the buses that correspond to the disturbance. That means if a load-shedding is applied at a load connected to bus X, the frequency and voltage response will be represented at bus X. Unlike the case of calculating load points when the demand is maximum inside Germany, In this case, the solar generation is present since the maximum demand occurs at 13:00 when there is solar radiation, which will contribute in the stability of the system since there is a large availability of synchronous machine power.

4.2.1 Disconnecting Synchronous Machine at Cluster 40003

In this scenario, the synchronous generator that is producing the largest amount of power (13.46 GW) is faulted at a time of 10 s and disconnected after 100 ms. In

Figure 37, the frequency response can be seen. Both systems can operate after a large disturbance in the steady-state region. The reason that the system without VSM was able to withstand the large disturbance is that there is high availability of solar generation. So the contribution of synchronous machines is lower. In the case of taking into consideration the maximum load only inside Germany, the same generator was generating a power of 20.36 GW which makes 25.45% of the total generation. But now, the power generated by the same generator makes 14.96% of the total generation. However, it can be seen that the OS, US, and RoCoF of the system with VSM are doing better than the system without VSM.

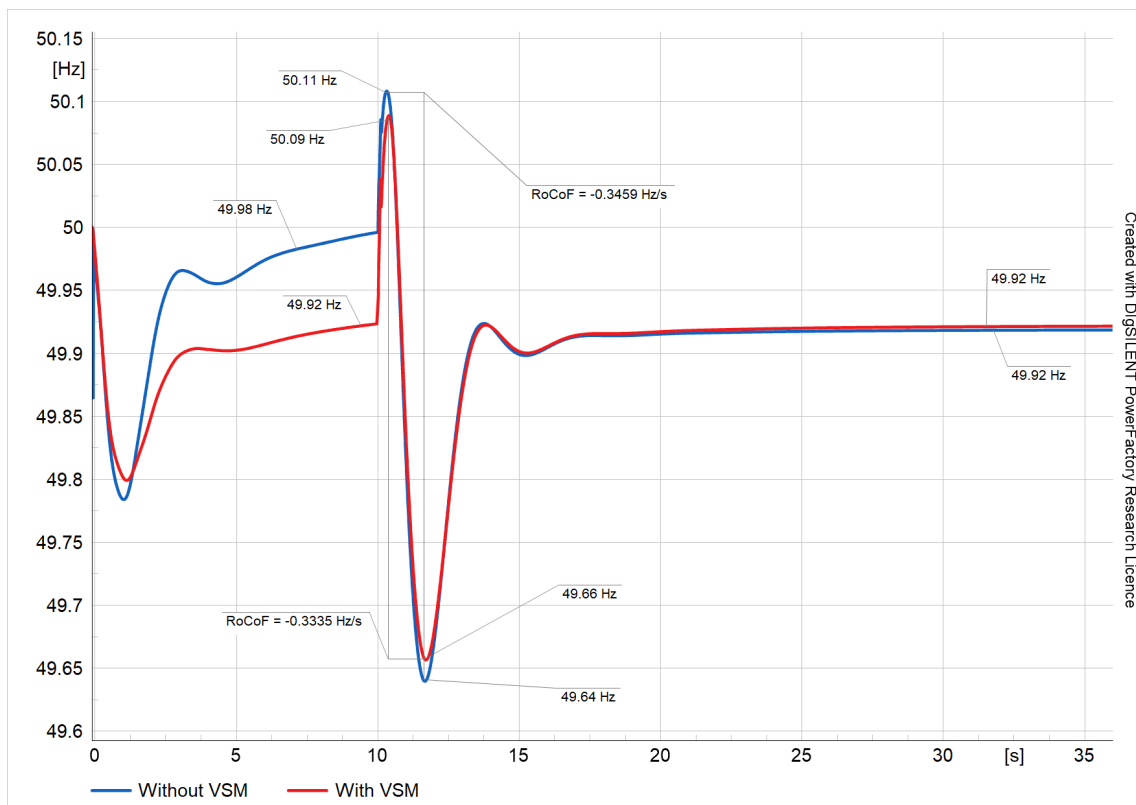


Figure 37: Frequency response for case 4.2.1

The voltage response is shown in Figure 38. It can be seen that the voltage drops to zero at cluster 40003 since it's shorted when the fault occurs, and then it restores its value to the steady-state operation. The performance of the two curves is very similar even in the FRT. There is a very slight difference in the FRT time between the two systems where the system with VSM is a little bit faster.

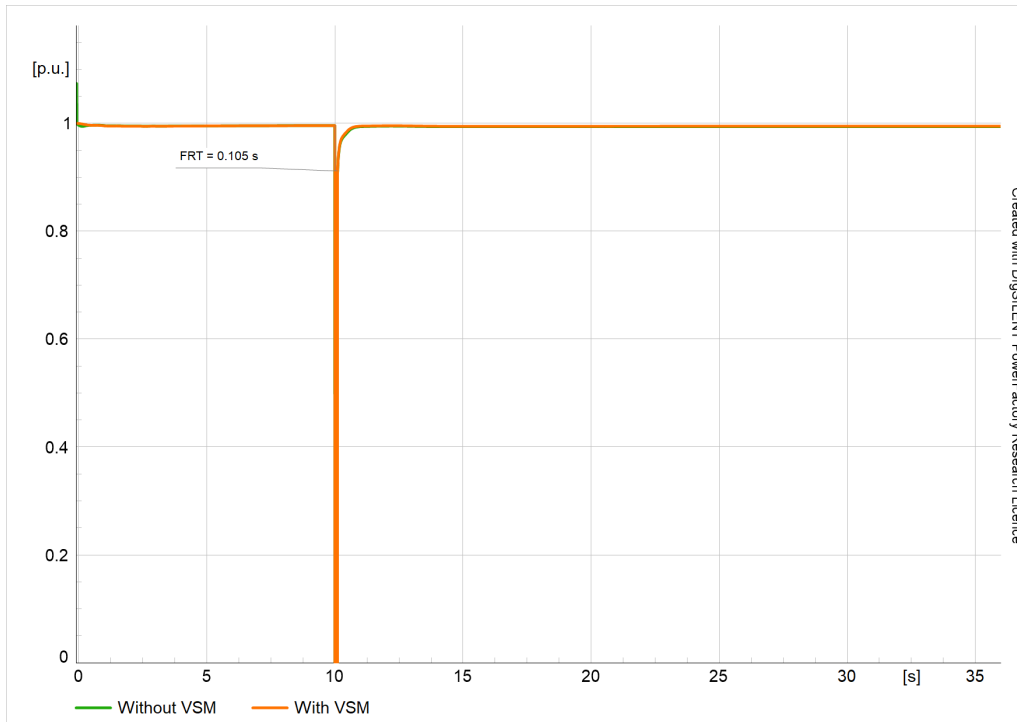


Figure 38: Voltage response for case 4.2.1

The Results of disconnecting the synchronous machine at cluster 40003 after a severe short-circuit fault are shown in Table 12.

Table 12: Results for case 4.2.1

| Quantity | VSM | No VSM |
|---------------|-------|--------|
| OS [Hz] | 50.09 | 50.11 |
| US [Hz] | 49.66 | 49.64 |
| RoCoF [Hz/s] | -0.33 | -0.35 |
| f_{ss} [Hz] | 49.92 | 49.92 |
| FRT [s] | 0.11 | 0.11 |

It can be seen from the results that all values including instantaneous values, RoCoF, and f_{ss} comply with the ENTSO-E grid code. Hence, no interruption or trip action will be taken [14].

4.2.2 Load-Shedding

Figure 39 shows the frequency response when shedding 9.26% of the total load at a time of 25 s at cluster 40007. The disturbance time is set to 25 s to show that the system is stable before the time of disturbance and its frequency settles. The value of this load is 8.8 GW and it is the load connected to cluster 40007. Both systems with and without VSM can recover from the load-shedding event. However, still, the OC, US, and RoCoF of the system with VSM outperform the system without VSM.

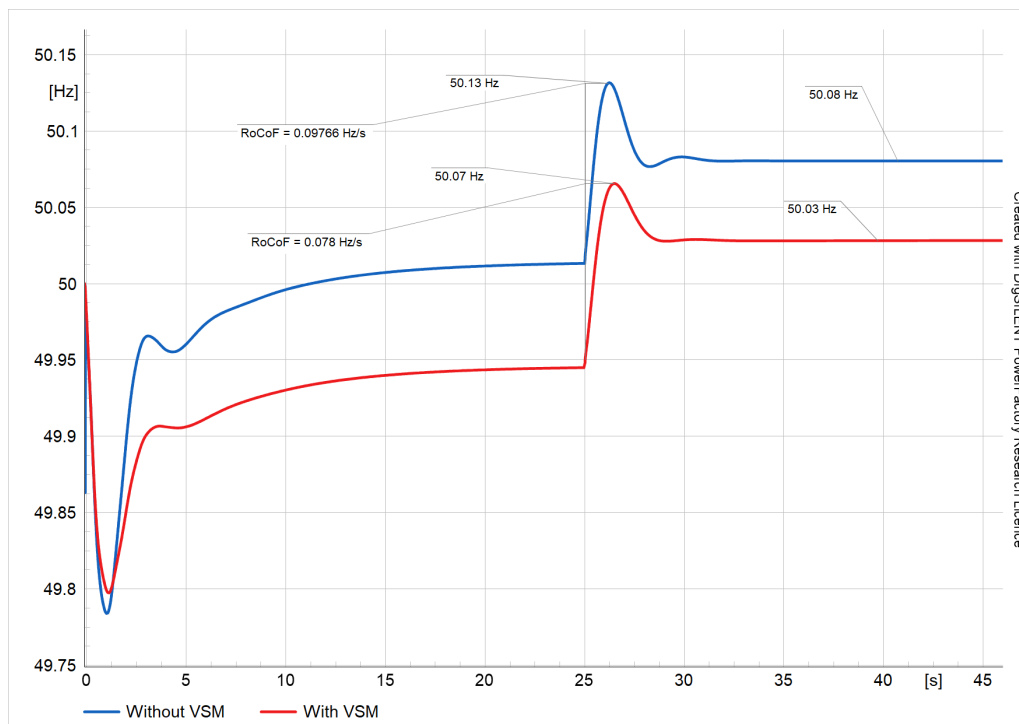


Figure 39: Frequency response at 9.26% load shedding of total load

The voltage response of the 9.26% load-shedding scenario is shown in Figure 40. It can be seen that the performance of the curves (with and without VSM) is very similar. Also, the reason for the voltage rise as mentioned before, is due to the decrease in the load current after disconnecting the load which leads to a lower voltage drop and lower reactive power consumed by the load that results in a higher voltage at the receiving end (bus 40007). The voltage is stable before, during, and after the disturbance.

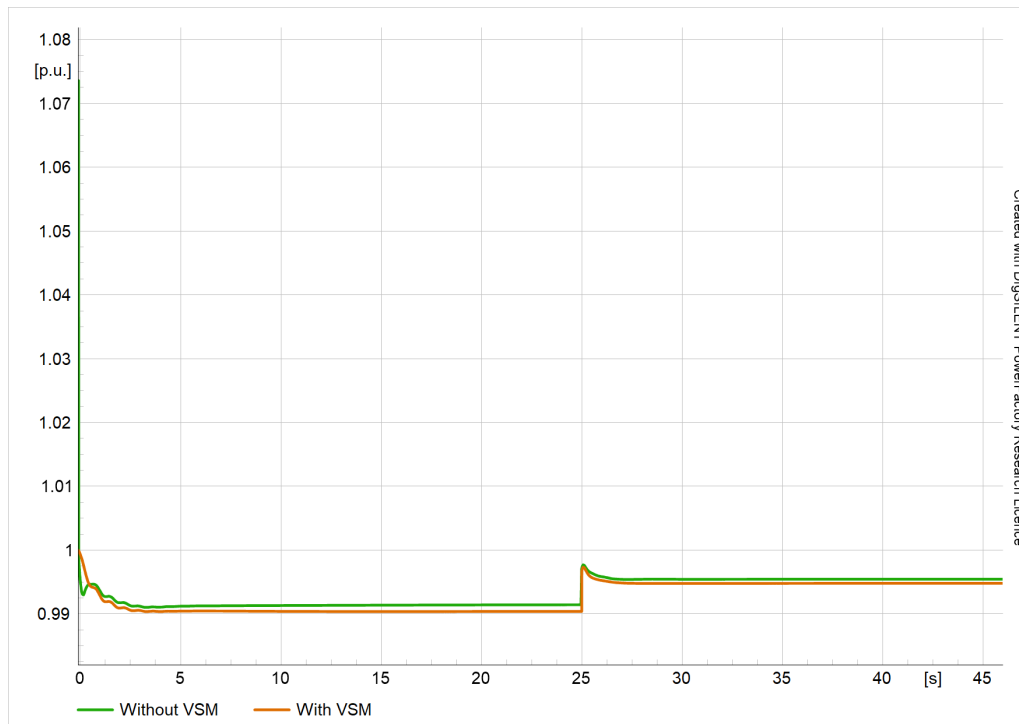


Figure 40: Voltage response at 9.26% load shedding of total load

The frequency response of a 13.46% load-shedding at cluster 40003 is shown in Figure 41. This load is located at cluster 40003 and its value is 13.68 GW. It can be seen in this scenario that the system with VSM is doing better than the system without VSM, especially after the disturbance where the system with VSM has a frequency closer to the nominal frequency than the system without VSM, but both operate within the stability limit. Also, the OS and RoCoF of the system with VSM are lower in value than the system without VSM which means better performance. In the literature, the system with VSM has to perform better than the system without VSM in case of load-shedding especially in the frequency response [7][27]. That verifies the results obtained in all load-shedding scenarios, whether the maximum total demand is taking into consideration the interconnectors that are going outside Germany or it is only considering the loads inside Germany. The voltage response of 13.46% load-shedding is shown in Figure 42. It can be seen that both curves act very similar and both curves do not leave the steady-state operational limits.

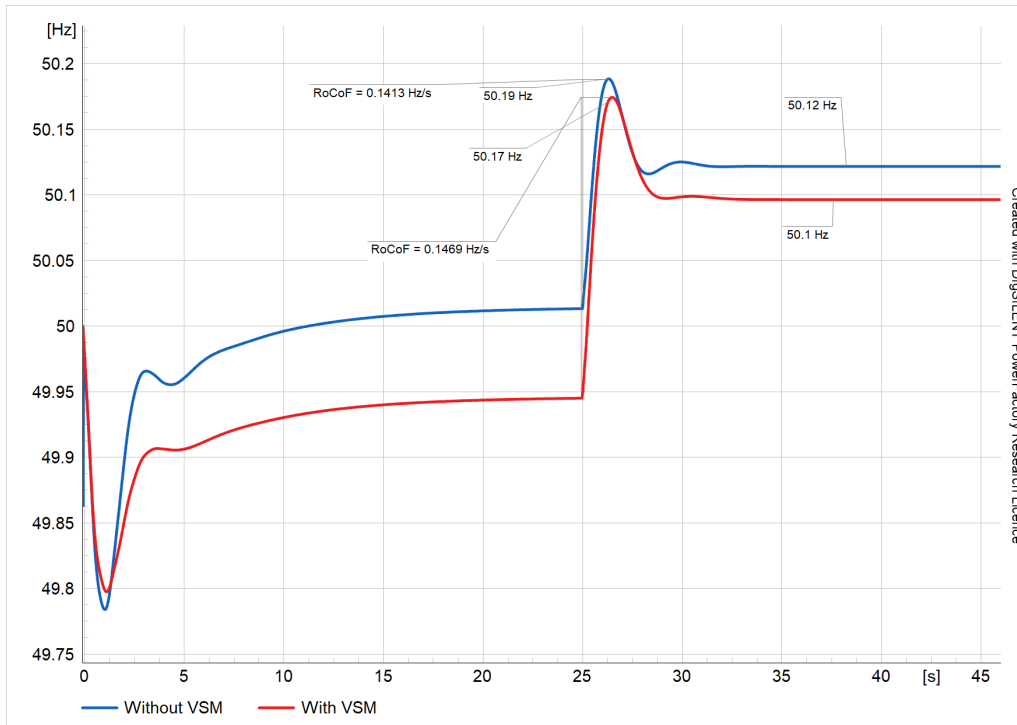


Figure 41: Frequency response at 13.46% load shedding of total load

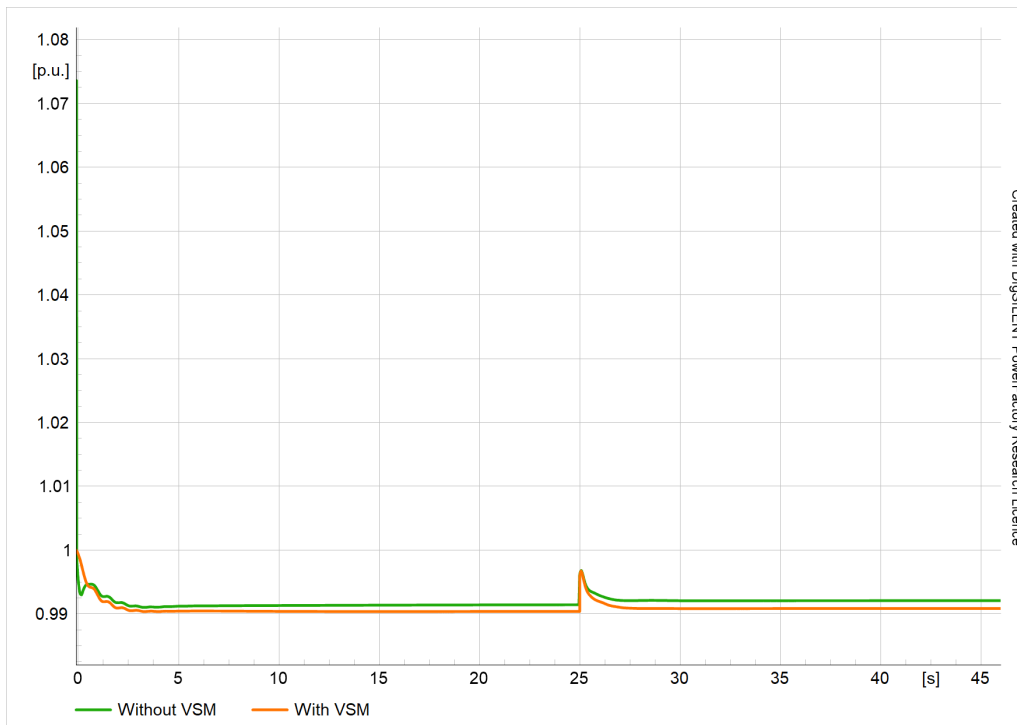


Figure 42: Voltage response at 13.46% load shedding of total load

The summary of 13.46% load-shedding results is shown in Table 13.

Table 13: Results for 13.46% load-shedding of total load

| Quantity | VSM | No VSM |
|---------------|-------|--------|
| OS [Hz] | 50.17 | 50.19 |
| RoCoF [Hz/s] | 0.15 | 0.14 |
| f_{ss} [Hz] | 50.1 | 50.12 |

From Table 13, it can be seen that all results comply with the ENTSO-E grid code. Also, as mentioned before and referring to the literature, it is expected from the system with VSM to outperform the system without VSM in the load-shedding scenario [7].

4.2.3 Disconnecting Line 40000-40001, 100 ms after a Short Circuit Fault in the Middle of the Line

Figure 43 shows the frequency response when disconnecting the highest-loaded transmission line in the system after suffering from a fault in the middle of line 40000-40001. The three-phase fault occurs at a time of 25 s, then both frequencies go through an overshooting and undershooting then stabilize at a frequency within the steady-state region. It can be seen that the red curve has less OS and less RoCoF from the OS to the US. Figure 44 shows the voltage response, as mentioned before, the voltage at buses 40000 and 40001 does not completely collapse and drop to zero. This is because the clusters are not completely shorted from the beginning of the line. Rather than that, the short circuit happens at the middle of the line which means that the voltage of each cluster at the moment of the fault is equal to the fault current multiplied by the impedance of half of the line. Afterwards, the voltage recovers in both systems (with and without VSM) and results in intact values. The FRT is almost the same for both systems. As said before, VSM plays a vital role in frequency response with no significant change in the voltage response.

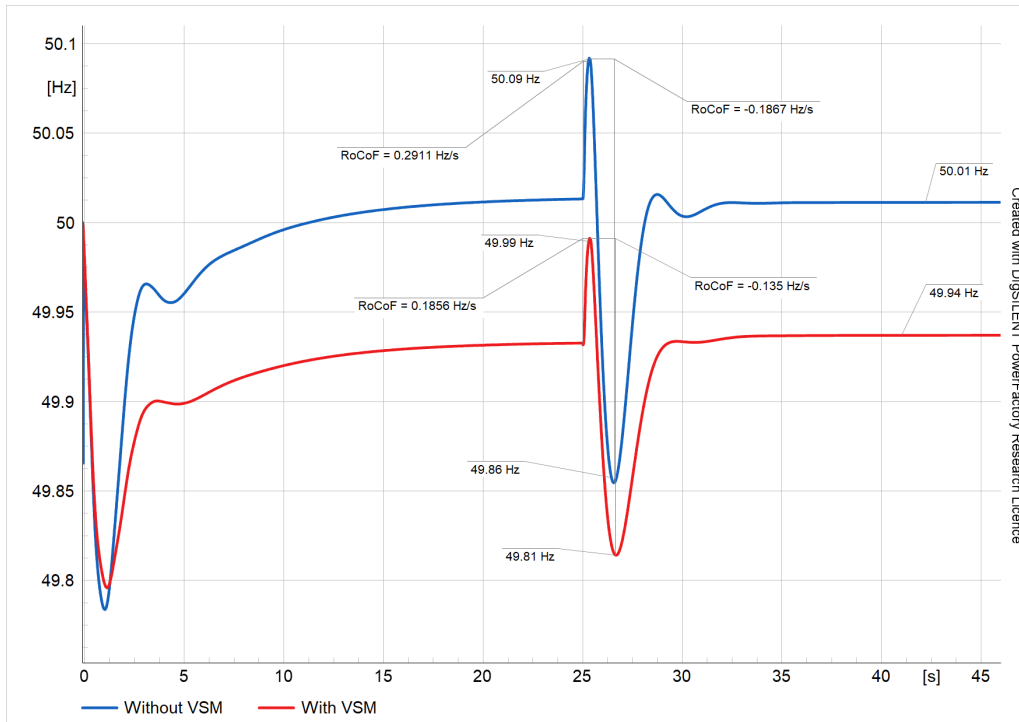


Figure 43: Frequency response for case 4.2.3

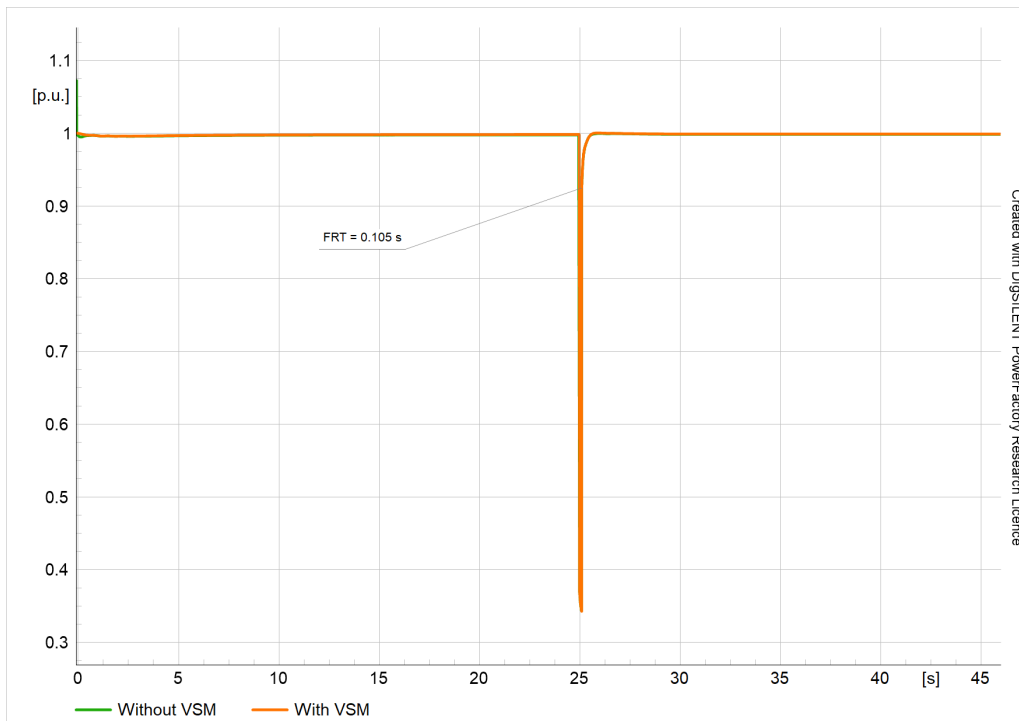


Figure 44: Voltage response for case 4.2.3

The results of short-circuiting and disconnecting the line 40000-40001 are shown in Table 14.

Table 14: Results for shorting and disconnecting line 40000-40001

| Quantity | VSM | No VSM |
|----------------|-------|--------|
| OS [Hz] | 49.99 | 50.09 |
| US [Hz] | 49.81 | 49.86 |
| RoCoF 1 [Hz/s] | 0.19 | 0.29 |
| RoCoF 2 [Hz/s] | -0.14 | -0.19 |
| f_{ss} [Hz] | 49.94 | 50.01 |
| FRT [s] | 0.11 | 0.11 |

From the results in Table 14, it is noticed that the results comply with the ENTSO-E grid code [14]. However, the system with VSM has better results than the one without VSM, especially the values of OS, US, and RoCoF.

4.3 Comparison between the Two Maximum Demand Cases

From the results in 4.1 and 4.2, it can be seen that at the time step of maximum demand considering loads outside Germany, the stability response of the system is generally better than at the time step when the maximum demand only inside Germany occurs, especially for the frequency response. This is because, at the time step of maximum demand taking into consideration loads only inside Germany, solar generation is not present since it occurs at 19:00 where there is no solar radiation, therefore the emulation of GFCs is only limited to wind generators which will reduce the role of GFCs and their contribution in bringing better frequency response.

5 Conclusion

The German Northwestern Grid, like many power systems networks worldwide, faces challenges in maintaining transient stability, especially in weak grids with a low short circuit ratio (SCR). In recent years, the industrial orientation has shifted towards utilizing grid-forming converters instead of grid-following converters, particularly to support weak grids. Among the controllers used in grid-forming converters are

Virtual Synchronous Machines (VSMs), which aim to emulate the behaviour of synchronous machines by injecting synthetic inertia (SI). This thesis investigated the impact of VSM penetration on transient stability and explored the potential benefits of grid-forming controllers in enhancing system performance.

The research approach starts with the construction of a comprehensive grid model under maximum demand conditions taking into consideration the moment of maximum demand only inside Germany, and also the maximum demand including interconnectors outside Germany. The German grid was represented by clusters, but the Northwestern German grid was represented with more details which is implemented in a higher number of clusters. Subsequently, the VSM, along with other essential controllers such as Load Frequency Control (LFC), Automatic Voltage Regulator (AVR), Power System Stabilizer (PSS), and other controllers used in renewable energy generators were incorporated and subjected to rigorous testing. Simulation scenarios for transient stability were performed both with and without VSMs to compare their effects on the system's performance. Data analysis using Python was used in order to aggregate generators and implement clusters, calculate the overall inertia constant H for the aggregated generators, aggregate loads and find the maximum demand point.

The results demonstrated that incorporating VSMs into the system significantly improved its transient stability, especially during challenging events such as load shedding and disconnection of transmission lines after a short circuit fault. The frequency response exhibited better performance in terms of steady-state frequency, overshooting (OC), undershooting (US), and Rate of Change of Frequency (RoCoF) with the presence of VSMs since they mimic the behavior of synchronous generators including inertia and damping. Also, synchronverter frequency response was tested for load shedding and it proved a stable performance similar to the VSM. These findings align with existing literature that primarily focuses on transient events involving load shedding and transmission line disconnection following a short circuit fault.

The study evaluated the compliance of the results with the ENTSO-E grid code, in most cases the behaviour of the systems complies with the ENTSO-E grid code. However, the system with VSM shows better performance than the one without VSM. The study also shows that the voltage response was somehow similar for systems with and without VSMs. This similarity can be attributed to the utilization of a PI voltage controller in the VSM, which aligns with the current voltage control strategies that are commonly employed. Nevertheless, the fault ride-through time (FRT) performed better in the system with VSMs.

Despite the promising results, the deployment of VSMs and grid-forming controllers still faces some challenges. For future studies it is also essential to refine

the grid model in a way that contains more details about the structure and connection of loads, lines, and generators to avoid any potential inaccuracies arising from approximations. Additionally, employing more sophisticated voltage controllers like PID in future studies could further improve the voltage response of the system since the voltage controller that is used in this research is a PI controller.

In order to continue advancing this research, it is recommended to employ specialized electromagnetic transient (EMT) simulation tools like PSCAD, renowned for their proficiency in EMT simulations [28]. This would facilitate investigating sub-synchronous oscillations of grid-forming converters and their controllers against synchronous generators, particularly regarding resonance stability which represents a serious issue because it causes rotors to oscillate where these oscillations of low frequency are slow and hard to dampen which might cause life-shortening or even damage in the rotor of the generator [29] [30].

On the one hand, this research focused more on the Northwestern part of the German grid from the perspective of modelling where the Northwestern part was modelled more precisely than the rest of the German grid by considering more details and a higher number of clusters which includes higher number and further distribution of loads, generators, and transmission lines. On the other hand, this research did not take into consideration implementing more penetration of wind and solar generators in the future in the Northwestern part of Germany and simulating their effect on the transient stability of the whole German grid. The reason for this is that implementing more generators requires modification on the current grid model where this will need more substations and transmissions lines and other components and the time available was not sufficient to do this localized analysis of the Northwestern region. For the future and once the prospective grid model is available, it can be done to focus on the transient stability of the Northwestern grid and its relevance to the deployment of VSMS in the prospective wind and solar generators.

Looking ahead, future research in this field should aim to explore the network restoration capabilities of grid-forming converters when working together with their controllers like VSM, especially in the aftermath of blackouts. It's still under investigation whether grid-forming converters and VSMS are capable of restarting a power system. Additionally, efforts should focus on addressing the challenges that still persist in grid forming controllers and VSMS, including developing a unified and optimized design for VSMS [29].

In conclusion, this thesis provides valuable insights into the potential of grid-forming converters, specifically VSMS, in enhancing transient stability in the German grid. The results clearly indicate that incorporating VSMS can significantly improve the system's frequency response during transient events, which is crucial for maintaining the overall stability of the grid. However, to fully exploit the benefits

of VSMS and grid-forming controllers, future studies should address the challenges mentioned and utilize advanced simulation tools, paving the way for a more resilient and efficient power grid in the German grid and beyond.

References

- [1] H. Saadat, *Power System Analysis*. McGraw Hill Series in Electrical and Computer Engineering, 1999.
- [2] M. Sarajlic, D. Peters, R. Beckmann, I. Liere-Netheler, F. Schuldt, and K. v. Maydell, "Application of open source models and data sets for energy system research: (user) experiences from ongoing and completed projects," in *2022 Open Source Modelling and Simulation of Energy Systems (OSMSES)*, (Aachen, Germany), pp. 1–6, 2022.
- [3] "Open_ego project website." <https://openenergyplatform.org>. Accessed: 07-08-2023.
- [4] Fraunhofer ISE, "Öffentliche nettostromerzeugung in deutschland im februar 2020." <https://www.energy-charts.info/charts/power/chart.htm?l=de&c=DE&interval=month&year=2020&month=02>. Accessed: 08-06-2023.
- [5] Fraunhofer ISE, "Öffentliche Nettostromerzeugung in Deutschland im Januar 2020." <https://www.energy-charts.info/charts/power/chart.htm?l=de&c=DE&interval=month&year=2020&month=01>. Accessed: 08-06-2023.
- [6] A. Abdelhay and L. Ntaimo, "Virtual inertia using grid-forming converters for enhancing the resilience of power systems," *IEEE Transactions on Industry Applications*, vol. 57, no. 5, pp. 5639–5653, 2021.
- [7] L. Arief, N. Hariyanto, and A. F. Maha, "Study of virtual synchronous machine (vsm) converter controller response on frequency and transient stability," in *2018 Conference on Power Engineering and Renewable Energy (ICPERE)*, pp. 1–6, 2018.
- [8] M. Yiwei, F. Wang, and L. Tolbert, "Virtual synchronous generator with limited current – impact on system transient stability and its mitigation," *2020 IEEE Energy Conversion Congress and Exposition (ECCE)*, 2020.
- [9] P. Li, Y. Wang, Y. Liu, H. Zhou, G. Gao, and W. Lei, "Transient stability analysis of virtual synchronous generator connected to an infinite bus," in *2019 IEEE Energy Conversion Congress and Exposition (ECCE)*, pp. 2099–2104, 2019.
- [10] Q. Zhong and G. Weiss, "Synchronverters: Inverters that mimic synchronous generators.," *IEEE Transactions on Industrial Electronics*, vol. 58, pp. 1259–1267, 2011.
- [11] S. D'Arco and J. A. Suul, "Equivalence of virtual synchronous machines and frequency droops for converter-based micro-grids," *International Journal of Electrical Power & Energy Systems*, vol. 5, pp. 394–395, 2014.
- [12] A. M. El-Zonkoly, A. F. Zobaa, and E. F. El-Saadany, "Network reduction techniques for power system analysis: A review," *Electric Power Systems Research*, vol. 105, pp. 145–158, 2014.
- [13] ENTSOE, "Network codes." https://www.entsoe.eu/network_codes/. Accessed: 28-07-2023.

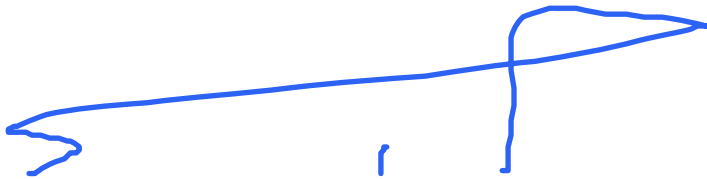
- [14] “ENTSO-E Grid Code, System Operations.” <https://eur-lex.europa.eu/legal-content/EN/TXT/?uri=CELEX:02017R1485-20210315>, 2021. Accessed: 29-07-2023.
- [15] ENTSO-E, “ENTSO-E Network Code for Requirements for Grid Connection Applicable to all Generators,” 2013.
- [16] “Why is peak demand a concern for utilities.” <https://www.advancedenergy.org/2018/03/13/why-is-peak-demand-a-concern-for-utilities>. Accessed: 06-08-2023.
- [17] ENTSO-E, Project Inertia Team, “FREQUENCY STABILITY IN LONG-TERM SCENARIOS AND RELEVANT REQUIREMENTS,” pp. 5–7, 2021.
- [18] W. Stevenson and J. Grainger, *Power System Analysis*. McGraw-Hill Education, 2011.
- [19] X. J. H. L. P. C. Wang, “Stability analysis and interaction of vsc grid-connected system under weak grid condition,” *IEEE*, vol. 4, 2023.
- [20] H. Zhao, L. Zhongcheng, L. Zhengyu, and X. Dianguo, “Control strategies for grid-forming inverters in renewable energy applications: A review,” *IEEE Transactions on Power Electronics*, vol. 36, pp. 4217–4231, 2021.
- [21] S. Eberlein and K. Rudion, “Small-signal stability modelling, sensitivity analysis and optimization of droop controlled inverters in lv micro-grids,” *International Journal of Electrical Power Energy Systems*, vol. 125, 2021.
- [22] A. Paquette and D. Divan, “Virtual impedance current limiting for inverters in micro-grids with synchronous generators,” *IEEE Transactions on Industry Applications*, vol. 51, pp. 1630–1638, 2015.
- [23] K. R. Padiyar, *Power System Dynamics: Stability and Control*. New Age International Publishers, 2010.
- [24] Q. Wu and S. Yuanzhang, *Power System Dynamics: Stability and Control*. New Age International Publishers, 2010.
- [25] “Digsilent powerfactory official website.” <https://www.digsilent.de/en/powerfactory.html>. Accessed: 07-08-2023.
- [26] B. Hartmann and G. Ódor, “Power-law distributions of dynamic cascade failures in power-grid models,” *Entropy*, 2020.
- [27] T. Kerdphol, M. Watanabe, Y. Mitani, D. Turschner, and H.-P. Beck, “Stability assessment of multiple virtual synchronous machines for microgrid frequency stabilization,” in *2020 IEEE Power Energy Society General Meeting (PESGM)*, pp. 1–5, 2020.
- [28] C. S. Heissel, G. Rogdakis, and P. J. Randewijk, “Comparative emt-simulations of energisation of transmission equipment for offshore wind farms,” in *2019 54th International Universities Power Engineering Conference (UPEC)*, p. 5, 2019.
- [29] T. MIDTSUND, A. BECKER, J. KARLSSON, and K. A. EGELAND, “A live black-start capability test of a voltage source hvdc converter,” *CIGRE*, vol. 676, 2015.
- [30] O. Adeuy, “Maximising hvdc support for gb black start and system restoration,”

- The National HVDC Center, Scotland*, vol. 2, 2019.
- [31] P. Kundur, *Power System Stability and Control*. McGraw-Hill Education, 1994.
 - [32] Burger, Andreas and Tzscheutschler, Peter and Schillings, Christoph and Pregar, Thomas and Sensfuss, Frank and Ragwitz, Mario, “Integration of renewable energy sources in Germany: a review,” *Renewable and Sustainable Energy Reviews*, vol. 82, no. 2, pp. 2873–2883, 2018.
 - [33] A. Jossen and A. Mertens, “Grid-forming converters,” *IEEE Journal of Emerging and Selected Topics in Power Electronics*, vol. 4, no. 4, pp. 1067–1076, 2016.

Declaration

I state and declare that this thesis was prepared by me and that no means or sources have been used, except those, which I cited and listed in the References section. The thesis is in compliance with the rules of good practice in scientific research of Carl von Ossietzky Universität Oldenburg.

Oldenburg, 10th of August 2023

A handwritten signature in blue ink, consisting of a long horizontal stroke with a small hook at the end, and a vertical stroke that loops back to the horizontal line.